

## **Forsmark site investigation**

### **Mapping of borehole breakouts**

**Processing of acoustical televieverdata  
from KFM01A, KFM01B, KFM02A, KFM03A,  
KFM03B, KFM04A, KFM05A, KFM06A  
and KFM07C**

Jørgen Ringgaard, Rambøll A/S

April 2007

**Svensk Kärnbränslehantering AB**  
Swedish Nuclear Fuel  
and Waste Management Co  
Box 5864  
SE-102 40 Stockholm Sweden  
Tel 08-459 84 00  
+46 8 459 84 00  
Fax 08-661 57 19  
+46 8 661 57 19



## **Forsmark site investigation**

### **Mapping of borehole breakouts**

**Processing of acoustical televewriterdata  
from KFM01A, KFM01B, KFM02A, KFM03A,  
KFM03B, KFM04A, KFM05A, KFM06A  
and KFM07C**

Jørgen Ringgaard, Rambøll A/S

April 2007

*Keywords:* Borehole breakouts, Televewriter, Deformations, Micro fallouts.

This report concerns a study which was conducted for SKB. The conclusions and viewpoints presented in the report are those of the author and do not necessarily coincide with those of the client.

Data in SKB's database can be changed for different reasons. Minor changes in SKB's database will not necessarily result in a revised report. Data revisions may also be presented as supplements, available at [www\(skb.se\)](http://www(skb.se)).

A pdf version of this document can be downloaded from [www\(skb.se](http://www(skb.se)

# **Abstract**

This report presents a detection and mapping of borehole breakouts and other borehole deformations by means of processing of data from an acoustical televiewer probe. Special attention is paid to very small breakouts and micro fallouts.

The registration is done in Excel-sheets in a table and a chart, which show the main azimuth of the breakouts. The charts show an obvious tendency, that the main azimuth of the breakouts and micro fallouts is found to be at 40 to 60° from magnetic north.

Due to the inclination of the boreholes, the televiewer is slightly decentralized during logging, which causes reduced data quality. But despite this, breakouts, keyseats and washouts with a certain magnitude (more than 0.1 mm), can still be mapped and classified after centralization of data by special processing routines.

Also micro fallouts (fallouts smaller than 0.1 mm) can be registered, but the mapping of these is more uncertain, as is it not possible to make specific criteria for this phenomenon. The detection has been done as a visual inspection and it is often hard to determine the area of distribution of these small structures. In some cases the micro fallouts are found to be in the entire perimeter of the borehole, but in most cases they have a main azimuth in the same direction as the breakouts.

With a perfect alignment of the BIPS-image in KFM01B the images complete each other, enabling an enhanced mapping of observed fractures and deformations.

## Sammanfattning

Denne rapport redovisar förekomsten och kartering av borrhålsspjälkning och andra borrhålsdeformationer, baserat på data från en akustisk televewersond. Särskild vikt har lagts vid mycket små borrhålsspjälkningar och mikroutfall.

Dataregistreringen är utförd i Excel-blad i tabeller och diagram, vilka illustrerar huvudazimuth för spjälkningarna. Diagrammen visar en tydlig tendens, att huvudazimuth för spjälkning och mikroutfall finns i intervallet 40–60° från magnetisk norr.

På grund av borrhålens lutning är televewersonden svagt decentralisera under loggningen, vilket leder till sämre datakvalitet. Trots detta är det möjligt att urskilja spjälkning, keaseats och washouts med bestämd magnitud (mer än 0,1 mm). Detta kan åstadkommas genom att centralisering kan göras genom en speciell dataprocessrutin.

Även mikroutfall (utfall mindre än 0,1 mm) kan urskiljas, men karteringen av dessa är mer osäker, då det inte är möjligt att precisera kriterium för detta. Urskiljning har kunnat göras genom visuell bedömning och ofta är det svårt att avgöra utbredningen av dessa. I några fall har mikroutfall förekommit i hela borrhålets perimetr, men i de flesta fall har de haft huvudazimuth i samma riktning som spjälkningen.

Med en perfekt inställning mellan loggen för televewern och BIPS-bilder i KFM01B, så kompletterar dessa varandra och möjliggör en förståelse/tolkning av observerade sprickor och deformationer.

# Contents

<b>1</b>	<b>Introduction</b>	7
<b>2</b>	<b>Objective and scope</b>	11
<b>3</b>	<b>Equipment</b>	13
<b>4</b>	<b>Processing of data</b>	15
4.1	Import and orientation	15
4.2	Alignment of images	15
4.3	Filtering and calculation of decentralization	16
4.4	Centralization of images	17
4.5	Calculation of calipers and ovality	17
4.6	Registration of breakouts and other deformations	22
4.7	Nonconformities	22
<b>5</b>	<b>Description of logpanel</b>	23
5.1	Explanation of logs	23
5.1.1	Amplitude	23
5.1.2	BIPS	23
5.1.3	Caliper max position	23
5.1.4	Caliper min position	23
5.1.5	Caliper – max – Centralized – Median filtered	23
5.1.6	Caliper – mean – Centralized – Median filtered	23
5.1.7	Caliper – min – Centralized – Median filtered	23
5.1.8	Class	23
5.1.9	Cross-section – Radius – Centralized	24
5.1.10	Decentralization	24
5.1.11	Radius – Centralized	24
5.1.12	Radius – Centralized – Median filtered	24
5.1.13	Radius – Centralized – Median filtered – median	24
5.1.14	Radius – Median filtered – max	24
5.1.15	Radius – Median filtered – median	24
5.1.16	Radius – Median filtered – mean	24
5.1.17	Radius – Median filtered – min	24
5.1.18	Tool rotation	24
<b>6</b>	<b>Analysis and registration of observed deformations</b>	25
6.1	Classification of observed deformations	25
6.2	Explanation of columns in the excel-sheet	25
6.3	Examples of borehole deformations	26
6.3.1	Example of borehole breakout (BB)	26
6.3.2	Example of washout (WO)	26
6.3.3	Example of keyseat (KS)	28
6.3.4	Example of micro fallout (MF)	28
6.4	Explanation of special features in the borehole	29
6.4.1	Tracks from decentralization	29
6.4.2	Drill cuttings from bottom of borehole	30
6.4.3	Wobbles from drilling process	30
<b>7</b>	<b>Summary and discussions</b>	33
	<b>References</b>	35

## **Appendices on CD**

**Appendix A** List of acquisition reports

**Appendix B** Tables and charts of depth errors

**Appendix C** Tables and charts of registered deformations

**Appendix D** Plot of logpanels

# 1 Introduction

Boreholes and tunnels in sedimentary formations as well as in bedrock may, during certain conditions governed by the relation between the compressive strength of the rock material and the state of stress, be exposed to spalling, often referred to as borehole breakouts, entailing that the originally circular borehole perimeter is deformed and changes its geometry to a more or less oval shape. (More exact definitions and a classification of borehole deformations of different types are given in Section 6.1.) The orientation of breakouts is governed by the stress field, such that the breakouts (ideally) occur on opposite sides of the borehole in the same bearing as that of the minor horizontal stress.

Width, length and depth of breakouts may vary within broad ranges, reflecting variations in the rock strength-/rock stress relation /Zoback et al. 1985/ and possibly also mirroring the impact of the drilling process /Ask et al. 2006/. The study of breakouts is primarily aiming at shedding light on the orientation of the stress field and its continuity. Secondarily, breakouts may be used also for determination of stress magnitudes, however mainly as a supporting method.

It has previously been shown that spalling phenomena may well be identified and characterized by the analysis of acoustic televiewer images /e.g. Deltombe and Schepers 2000, Siddans and Worthington 2003/. Due to the high accuracy of the acoustic televiewer method for determination of geometrical properties of the borehole, it is especially advantageous when addressing minor deformations, which may be very difficult to detect with other methods.

A pilot study aiming at investigating the potential of the acoustic televiewer method of identifying and characterizing major as well as minor borehole deformations in the rock types prevailing at Forsmark was performed during 2005 /Ask and Ask 2007, Ask et al. 2006/. Two subvertical core drilled boreholes, KFM01A (1,000 m long) and KFM01B (500 m) were investigated. The applicability of the method was clearly demonstrated and a range of borehole deformations of different dimensions was revealed in both boreholes. A pilot study was also performed by /Ringgaard 2006/.

This document reports the results gained by processing and interpretation of acoustic televiewer data from nine boreholes at Forsmark, which is one of the activities performed within the site investigation at Forsmark. The work was carried out in accordance with activity plan AP PF 400-06-062, see Table 1-1. Activity plans and method descriptions are SKB's internal controlling documents. However, for the activity presented in this report, there exists no SKB method description.

A map of the Forsmark investigation area is presented in Figure 1-1, whereas details of the different drill sites are shown in Figure 1-2.

Original data from the reported activity are stored in the primary database Sicada. Data are traceable in Sicada by the Activity Plan number (AP PF 400-06-062). Only data in databases are accepted for further interpretation and modelling. The data presented in this report are regarded as copies of the original data. Data in the databases may be revised, if needed. Such revisions will not necessarily result in a revision of the P-report, although the normal procedure is that major revisions entail a revision of the P-report. Minor revisions are normally presented as supplements, available at [www.skb.se](http://www.skb.se).

**Table 1-1. Controlling document for performance of the activity.**

Activity plan	Number	Version
Detection of potential borehole breakouts in boreholes KFM01A, KFM01B, KFM02A, KFM03A, KFM03B, KFM04A, KFM05A, KFM06A and KFM07C.	AP PF 400-06-062	1.0

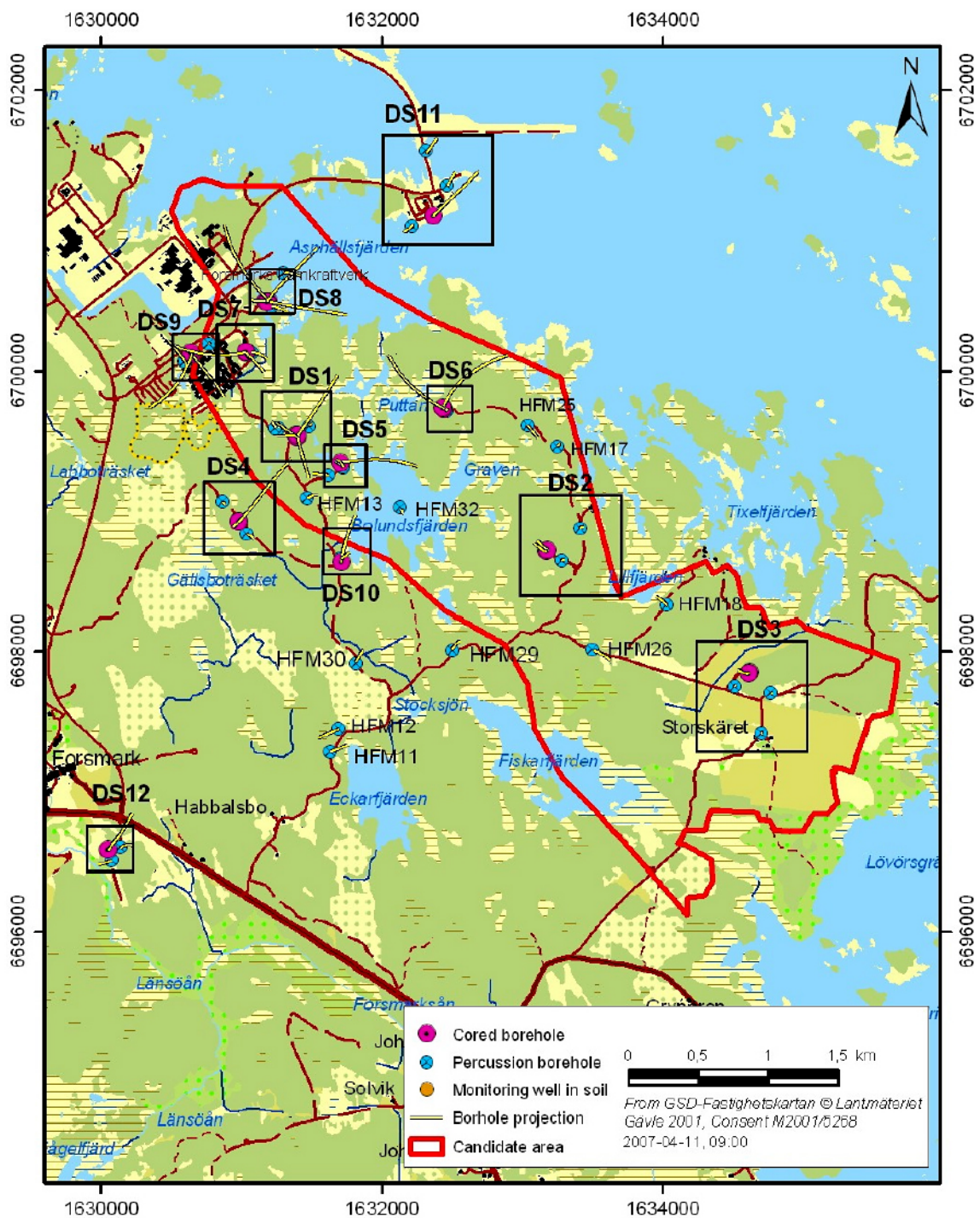


**Figure 1-1.** Map of borehole locations at the Forsmark investigation area.

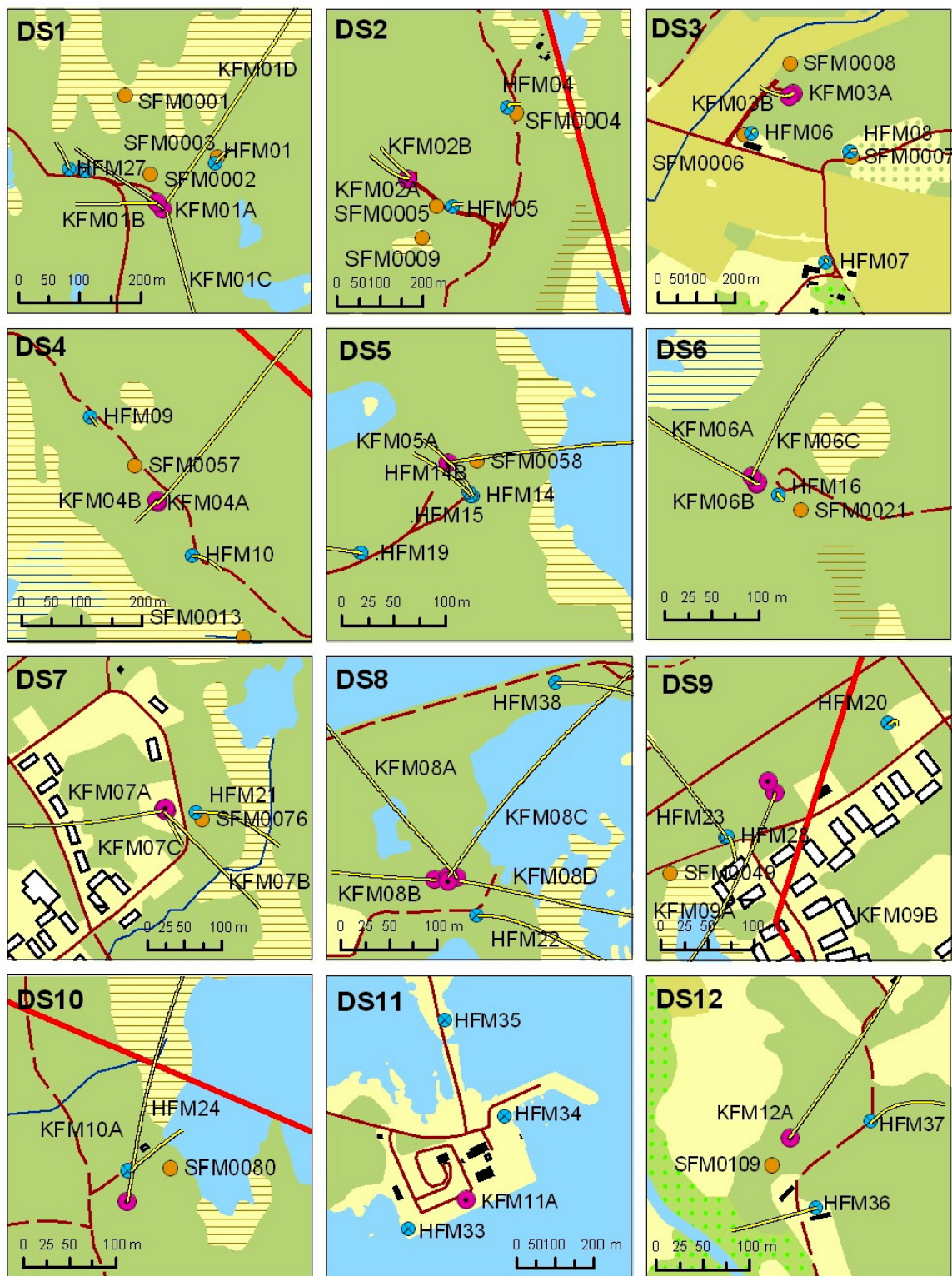


**Figure 1-2.** Detailed maps of the different drill sites.

## 2 Objective and scope

Efforts to map the effects of the stress in the Forsmark region have been done with a suite of methods. This report describes a special processing of televIEWer data with attention to the effect of stress: deformations of the borehole. The mapping is done according to the SKB-document AP PF 400-04-062. An overview of the processed boreholes can be found in Table 2-1.

**Table 2-1. Overview of boreholes (from SICADA).**

Borehole	Length [m]	Inclination [° from hor.]	Orientation [° from GN]
KFM01A	1,001	-84.73	318.35
KFM01B	500.52	-79.04	267.59
KFM02A	1,002.44	-85.38	275.76
KFM03A	1,001.19	-85.75	271.52
KFM03B	101.54	-85.30	264.49
KFM04A	1,001.42	-60.08	45.25
KFM05A	1,002.71	-59.80	80.90
KFM06A	1,000.64	-60.25	300.92
KFM07C	500.34	-85.40	98.39

### 3 Equipment

The probe used for acquisition of data is a High Resolution Acoustical Televiwer (HiRAT) from Robertson Geologging Ltd. <http://www.geologging.com/>

The transducer is a 1.5 MHz head, which transmits the acoustic signal via a rotating acoustic mirror to the borehole wall. The strength of the reflected signal is recorded as an Amplitude log, while the first arrivals are picked and stored in a Traveltime log. Both logs are stored as images with selectable horizontal resolution from 90 to 360 pixels/revolution and a vertical resolution depending on the logging speed. The radial resolution in the recorded Traveltime is 100 nS, which equals 0.075 mm. The boreholes were logged with different selections of resolution; an overview of this is shown in Table 3-1.

The images are oriented by means of a built-in orientation unit containing a 3-axis fluxgate magnetometer as well a 3-axis accelerometer. The output from this device can also be used to calculate a deviation log for the borehole.

The probe is centralized in the borehole with two bow spring centralizers, see the picture in Figure 3-1. The applied centralizers are designated to boreholes with diameters in the range 67–100 mm.

For detailed information regarding the data acquisition with the HiRAT probe, please refer to SKB reports listed in Appendix A.

The BIPS-image (only in KFM01B) is recorded with the BIPS-system. For information regarding this probe and the acquisition of data; please refer to the SKB report P-05-74: RAMAC and BIPS logging in borehole KFM01B and RAMAC directional re-logging in borehole KFM01A.

**Table 3-1. Overview of resolutions.**

Borehole	Pixels/rev.	Horizontal res. [mm]	Logging speed [m/min]	Vertical res. [mm]
KFM01A	120	2.0	2	2
KFM01B	180	1.3	2	2
KFM02A	120	2.0	2.4	2
KFM03A	120	2.0	2.4	2
KFM03B	120	2.0	2.5	2
KFM04A	120	2.0	2.4	2
KFM05A	120	2.0	2.4	2
KFM06A	90	2.7	10	8
KFM07C	180	1.3	2	2



**Figure 3-1.** Picture of HiRAT probe.

## 4 Processing of data

The final processing of the televIEWER-data contains the steps described below. A lot of effort has been spent to investigate different possibilities in the processing. Only the final processing done to the delivered data is described. All processing is done in WellCAD, which is made by Advanced Logic Technology. A free reader for WellCAD documents can be downloaded on [www.alt.lu](http://www.alt.lu).

### 4.1 Import and orientation

The televIEWER data are recorded in the dedicated logging-program HiRAT from Robertson Geologging Ltd. The data are stored in time domain, with a table which links the data to depth.

Image-data as well as orientation-data are imported and resampled to depth-domain. Orientation-data are filtered with a 200 samples moving average filter. Images are resampled to 360 pixels/rev. before orientation. This is done to prevent fractures from being edged during orientation.

Images are then oriented to Magnetic North (MN).

### 4.2 Alignment of images

In order to provide a system for length calibration of different logging systems used at the site investigation, reference tracks (grooves) have been milled into the borehole wall with a specially designed tool at regular levels in all cored drilled boreholes. Regarding televIEWER logging, the length calibration is conducted as follows.

First all HiRAT logs are shifted, so that the upper edge of the top-most track is aligned to the milled reference track. Then all tracks in the borehole are identified and a table is made. An example of this is shown in Table 4-1.

**Table 4-1. Example of depth table. KFM01A.**

True depth [m]	HiRAT [m]	Difference [m]
110	110	0
150	150.041	-0.041
200	200.063	-0.063
250	250.109	-0.109
300	300.136	-0.136
350	350.149	-0.149
400	400.209	-0.209
450	450.202	-0.202
500	500.257	-0.257
550	550.258	-0.258
600	600.3	-0.3
650	650.327	-0.327
700	700.322	-0.322
750	750.359	-0.359
800	800.352	-0.352
1,000.5	1,000.96	-0.46

Also a plot of the differences is made. This is done to check the linearity of the depth fault, an example of a plot is shown in Figure 4-1. The depth tables and plots of all boreholes can be found in Appendix B.

All logs are then stretched to fit the milled tracks in the borehole, which results in a perfect alignment to the tracks.

### 4.3 Filtering and calculation of decentralization

To calculate the decentralization, the Traveltime image needs to be filtered with a  $15 \times 15$  pixels weighted average filter. This is done to prevent small fractures from disturbing the decentralization calculation. Then the image is converted from Traveltime (the unit is 100 nS) to radius with the formula:

$$\text{Radius(mm)} = \frac{(\text{Traveltime} - \text{Internal Traveltime} \times 10) \times \text{VEL(FL)}}{10 \times 1000} + \text{tool radius}$$

where “VEL(FL)” is the sound velocity in the borehole fluid.

“Internal Traveltime” is the internal traveltimes in the oil from the transducer to the acoustic window of the HiRAT tool. As the sound velocity in the oil has a small temperature coefficient, it is calculated as:

$$\text{Internal Traveltime} = \frac{(-2.24 \times \text{TEMP(FL)} + 1031) \times 120}{1000}$$

“TEMP(FL)” is the temperature of the water in the borehole, which was measured with a 9042 FluidRes and FluidTemp probe from Century Geophysical (see overview of acquisition reports in Appendix A). Also VEL(FL) is calculated in the reports, from the measured resistivity of the fluid.

Next step is to extract statistics from the new radius image log, which returns logs for minimum, maximum, average and median values of the radius image. From these the decentralization of the probe is calculated as:

$$\text{Decentralization} = \text{“Radius - mean”} - \text{“Radius - min”}$$

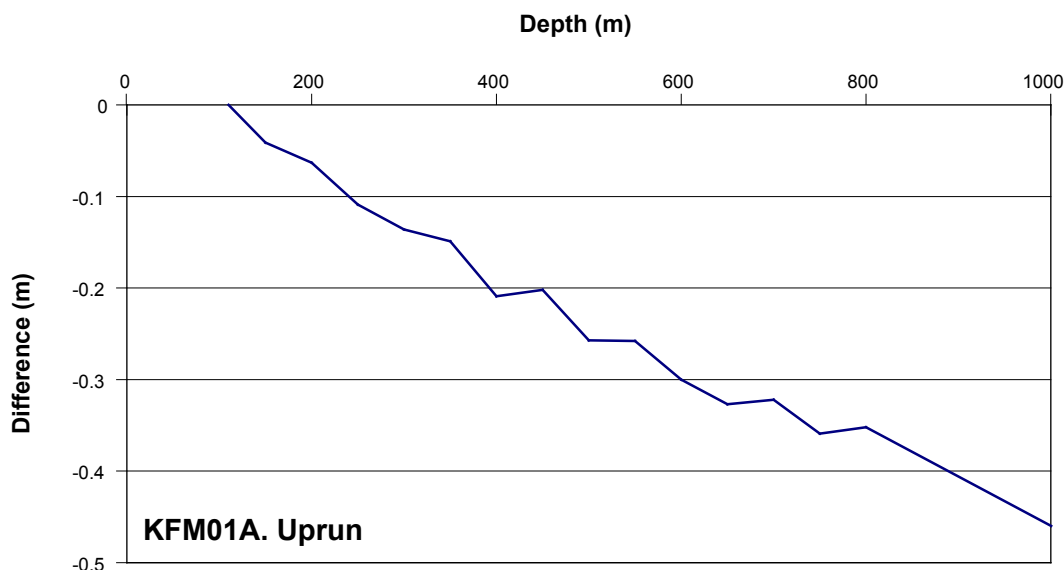


Figure 4-1. Example of plot of depth error: KFM01A.

## 4.4 Centralization of images

Due to the inclination of the boreholes, the acoustic televue-probe is slightly decentralized during logging; the size of this decentralization is roughly 0.1 mm/deg. from vertical. Therefore a centralization routine is applied to compensate the images for this. This is done by means of a sine-fitting routine in WellCAD. It can be done only to the Traveltime (Radius) image, not to the Amplitude image. In Figure 4-2, an example of an unrolled Radius curve at 121.32 m in KFM01B is shown, where the decentralization reaches a local peak, i.e. 0.96 mm.

In Figure 4-3 the same section as in Figure 4-2 is shown, but after the centralization routine has been applied. The images have been centralized, but also some distortion has been added to the image. The distortion is at worst, where larger breakouts are present. The centralization routine is applied both to the Traveltime image as well as the median filtered Radius image. In Figure 4-4 and Figure 4-5 examples of the effect of the centralization routine are shown at a depth, where the decentralization is at a local minimum, i.e. 0.11 mm.

**Please note**, that the scales of the un-rolled radius are different, i.e. 37 to 40 mm in the examples before centralization vs. 38 to 38.5 mm on the two examples after.

There are two types of overlaying decentralizations; the first type is as expected against the low side of the borehole. But a second type of decentralization is also present, which follows the rotation of the tool during logging.

## 4.5 Calculation of calipers and ovality

The Centralized Traveltime is then also converted to a radius image as described in 4.3 and the previous image is deleted.

Now mean, minimum and maximum calipers as well as angles (eg. Cal Max Position) for these can be extracted from the median filtered image log. Then the extracted angles (position logs) are filtered again with a 100 pts. (2 metres) moving average filter; this is done to smoothen the logs as only main angles are of interest.

An ovality log can now be calculated as twice the median radius minus the minimum caliper.

$$OVALITY - MIN = "Radius - Centralized - Median filtered - median" \times 2 - "Caliper - min - Centralized - Median filtered"$$

This ovality log will only be reliable where some ovality is present, as it will be smeared by the fractures in the borehole as well as method introduced artefacts. It also needs to be compared with the angle logs, which should be stable in one direction, before a eventual ovality can be considered reliable.

As a manual check of the ovality, cross-section logs are generated every 20 metres, as well as right above and below breakouts (the latter are deleted again). These cross-sections have grid-circles every 0.1 mm, allowing the ovality to be visually checked, see example in Figure 4-6 below.

The same process is applied to the downrun and imported to the uprun logpanel. It is used in case of doubt to help separating real deformations from artefacts. The Radius image from the downrun is part of the delivered logpanel, but not shown.

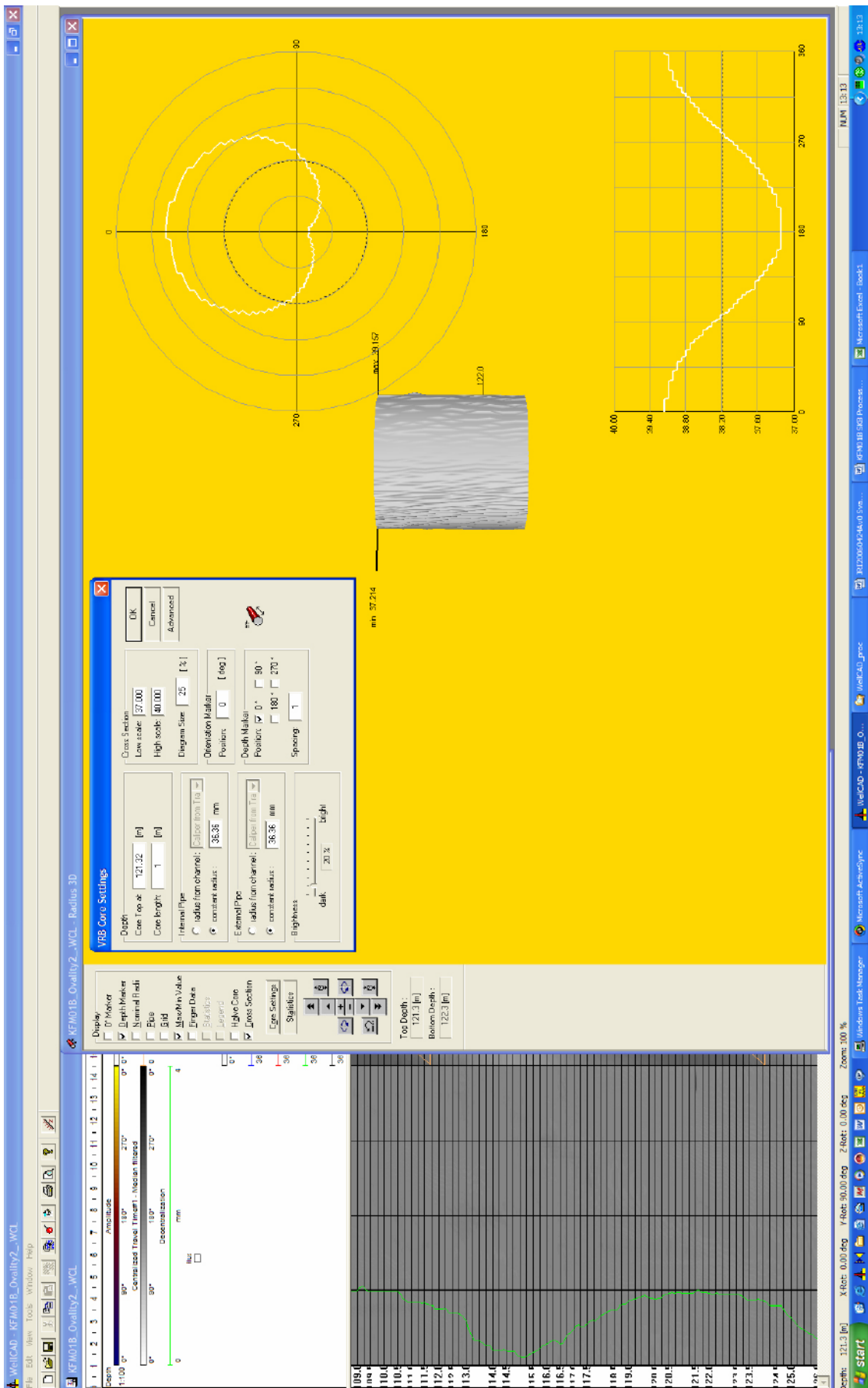
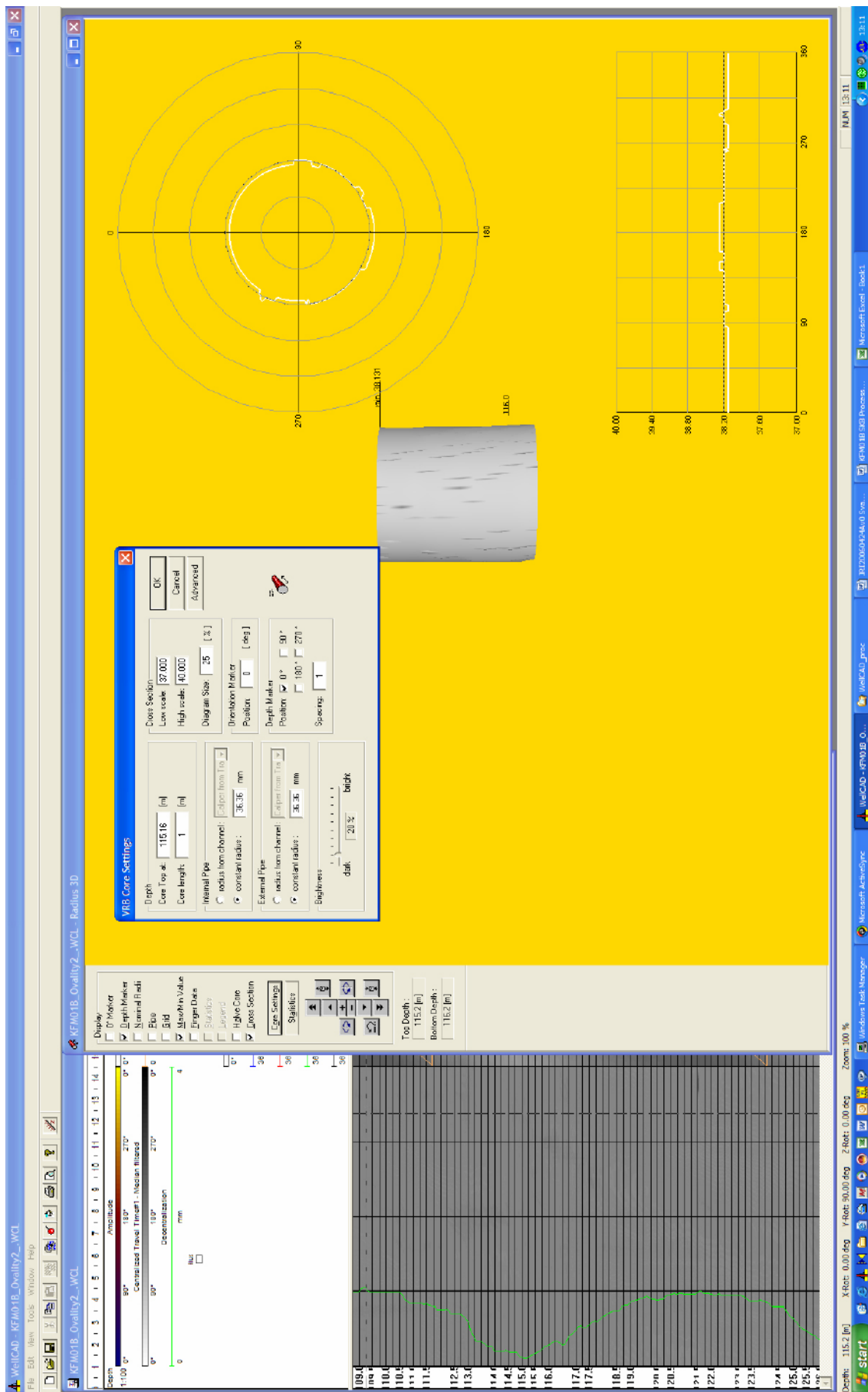


Figure 4-2. Example of maximum decentralization – at 121.32 m in KFM01B.



**Figure 4-3.** Example of maximum decentralization – at 121.32 m in KFM01B – after application of the centralization routine.

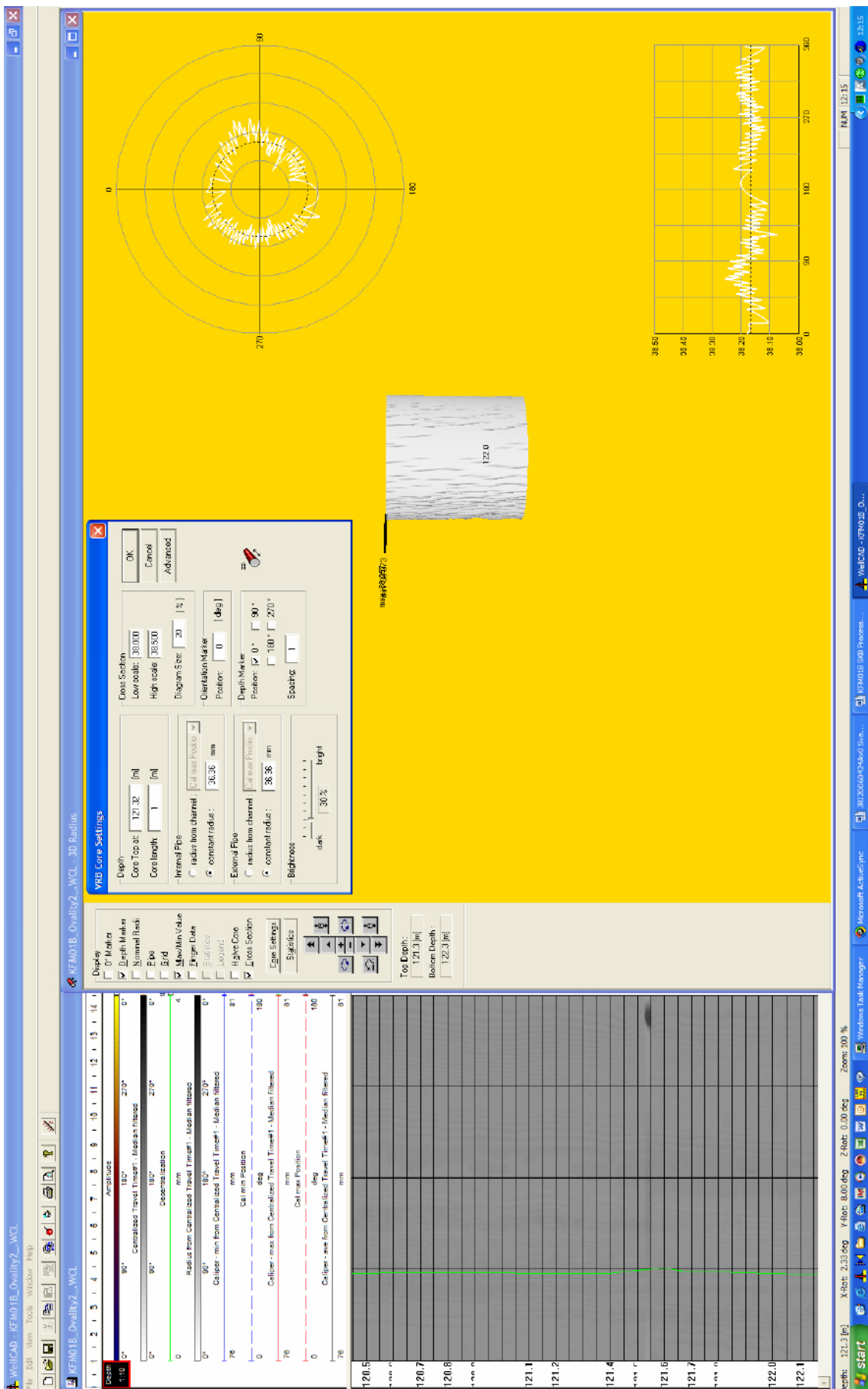
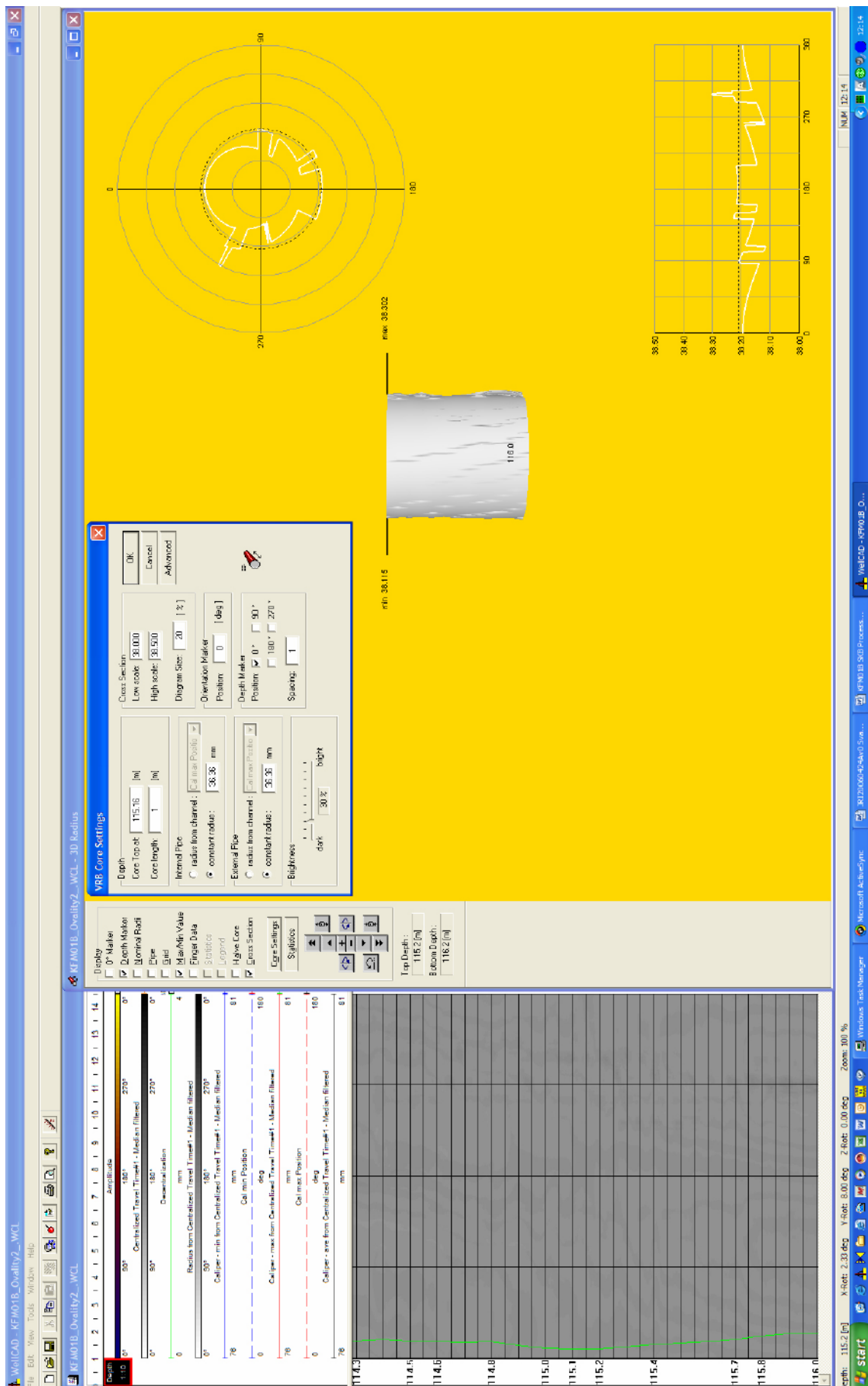


Figure 4-4. Example of minimum decentralization – at 115.16 m in KFM01B.



**Figure 4-5.** Example of minimum decentralization – at 115.16 m in KFM01B – after application of the centralization routine.

## 4.6 Registration of breakouts and other deformations

To register and describe deformations the log panel is manually inspected. When necessary a cross-section is generated and the deformation is classified, measured and registered in an Excel-table. In Figure 4-6 below is shown a example of a cross-section. The spacing between the radial grid is 0.1 mm. The spikes on the cross-section, which have a maximum size of 0.3 mm, show some roughness on the borehole wall – micro fallout.

## 4.7 Nonconformities

The activity was performed in compliance with activity plan AP PF 400-06-062, although with one exception. Analysis of borehole KFM07C was not included in the activity plan. However, a decision was made after approval of the activity plan, that the activity should encompass also KFM07C.

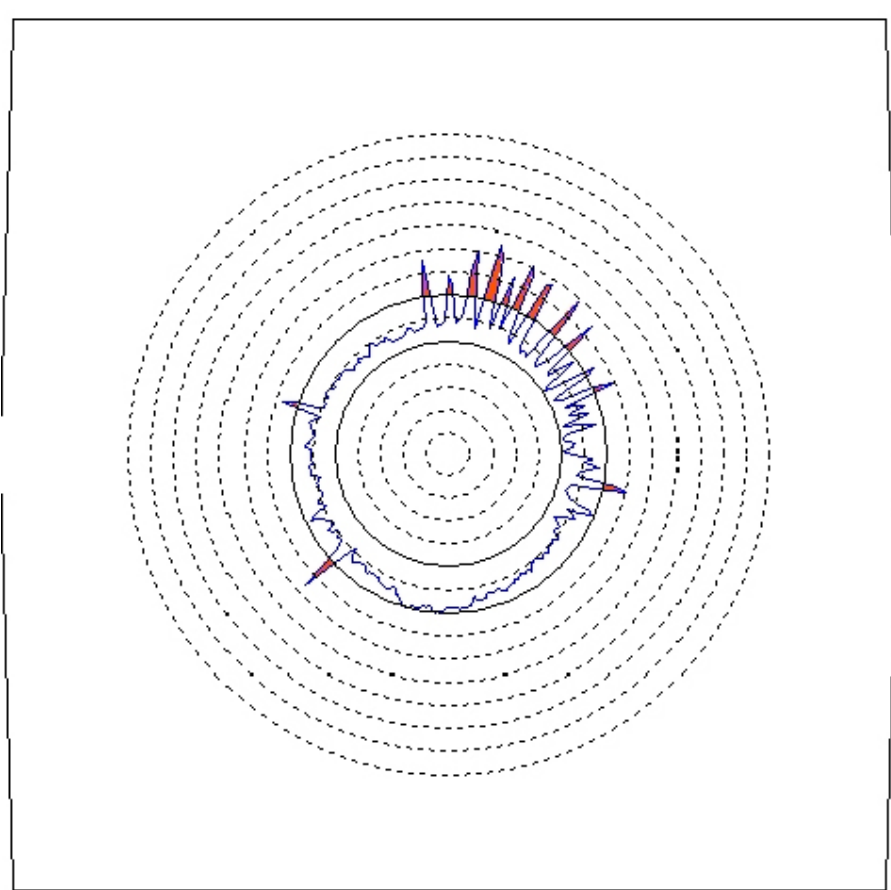


*Figure 4-6. Example of cross-section with micro fallout.*

## 5 Description of logpanel

### 5.1 Explanation of logs

Here follows – in alphabetic order – a description of all the logs in the panel

#### 5.1.1 Amplitude

Amplitude of the returned acoustic signal from the borehole wall. Darker (more blue) colours represent low amplitude – softer surface, while lighter (more yellow) colours represent high amplitude – harder surface of wall. The log is (as all other images) shown as an un-rolled 360° image of the borehole, where 0° is the reference, which is aligned against magnetic north (MN). The image is has no unit.

#### 5.1.2 BIPS

Image RGB-log from BIPS optical televiewer, (only in KFM01B).

#### 5.1.3 Caliper max position

Orientation of the calculated maximum caliper in degrees from MN of the borehole. The log is derived from the filtered and centralized radius image. Contains values from 0–180 degrees.

#### 5.1.4 Caliper min position

Orientation of the calculated minimum caliper in degrees from MN of the borehole. The log is derived from the filtered and centralized radius image. Contains values from 0–180 degrees.

#### 5.1.5 Caliper – max – Centralized – Median filtered

Maximum caliper measured in the median filtered and centralized radius image. Unit: mm.

#### 5.1.6 Caliper – mean – Centralized – Median filtered

Mean caliper measured in the median filtered and centralized radius image. Unit: mm.

#### 5.1.7 Caliper – min – Centralized – Median filtered

Minimum caliper measured in the median filtered and centralized radius image. Unit: mm.

#### 5.1.8 Class

Symbol log, which shows the classification of registered deformations. This log is pasted from the column in the registration excel-sheet.

BB		Borehole Breakout
KS		Key Seat
MF		Micro Fallout
WO		Washout

### **5.1.9 Cross-section – Radius – Centralized**

Cross-sections are generated every 20 metres in the borehole. The cross-section is average over 10 cm. Radii below the actual nominal radius are shaded green, and radii above are shaded orange.

### **5.1.10 Decentralization**

Calculated decentralization as the difference between the mean and min radius of the radius image. Unit: mm.

### **5.1.11 Radius – Centralized**

Radius image log, which is centralized as described to compensate for decentralization of the probe. Light colours represent smaller radii, while darker colours represent larger radii. Unit: mm.

### **5.1.12 Radius – Centralized – Median filtered**

Radius image log, which is centralized as described earlier and median filtered over an area of  $15 \times 15$  pixels (app.  $20 \times 30$  mm) to shade for small deformations, when calculating calipers. Light colours represent smaller radii, while darker colours represent larger radii. Unit: mm.

### **5.1.13 Radius – Centralized – Median filtered – median**

This log is not shown; it is used to calculate the ovality as described in Section 4.5.

### **5.1.14 Radius – Median filtered – max**

Maximum radius of the median filtered, but not centralized radius image, unit: mm.

### **5.1.15 Radius – Median filtered – median**

Median radius of the median filtered, but not centralized radius image, unit: mm.

### **5.1.16 Radius – Median filtered – mean**

Mean radius of the median filtered, but not centralized radius image, unit: mm.

### **5.1.17 Radius – Median filtered – min**

Minimum radius of the median filtered, but not centralized radius image, unit: mm.

### **5.1.18 Tool rotation**

Shows the rotation of the probe, as the borehole was logged, unit: degrees.

## 6 Analysis and registration of observed deformations

### 6.1 Classification of observed deformations

In Appendix C is found tables with classification of all interpreted deformations in the boreholes.

The classification is illustrated in Figure 6-1.

### 6.2 Explanation of columns in the excel-sheet

The columns in the Excel-sheet are explained as follows:

**Top Depth:** Top of the deformation.

**Bot. Depth:** Bottom of the deformation.

**Max. R:** Maximum radius of the deformation, read from “Radius – max – Median Filtered”-log and/or “Radius” image.

**Median R:** Nominal radius at the depth, read from “Radius – median – Median Filtered”-log.

**dRmax:** Delta radius, i.e. the depth of the deformation into the borehole wall.

**Structure:** Classification of the deformation. Examples and further explanation are shown in Section 6.3

BB: Borehole breakout

WO: Washout

KS: Key seat

MF: Micro fallout

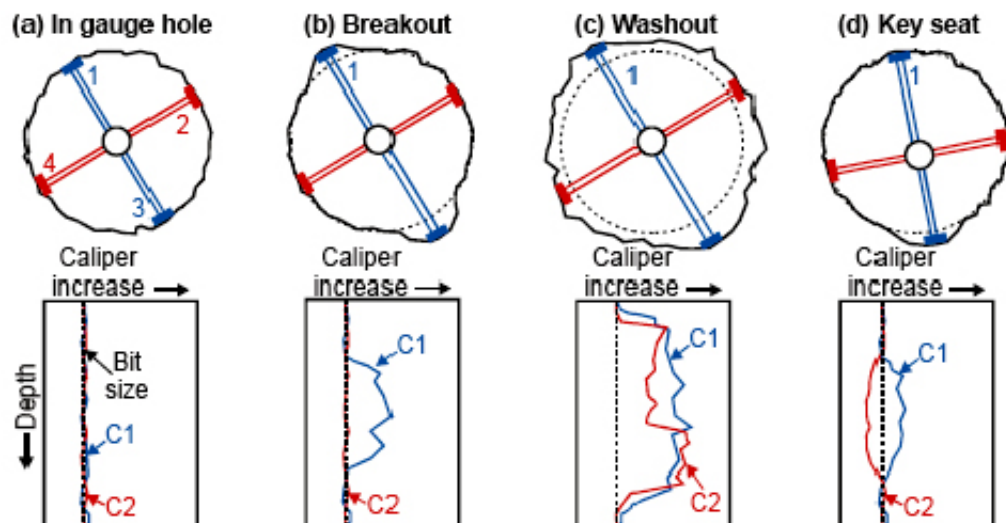


Figure 6-1. Classification of deformations. From /Ask and Ask 2007/, after /Plumb and Hickman 1985/.

**Uncertainty:** The uncertainty of the observed deformation: 3 = certain, 2 = probable, 1 = possible, 0 = not estimated. The uncertainty is primary related to the type of deformation.

**Cross. struct.:** The deformation is related to a fracture crossing the borehole. Example of this is shown in Section 6.3.

**Main azimuth:** Main azimuth of the deformation in degrees from Magnetic North. The angle is calculated from the next column “Azimuth”. If the angle is between 0 and 180°, the main azimuth is the same, but if the azimuth is between 180 and 360°, 180° are subtracted from the angle. Example of this is shown and explained in Section 6.3.

**Azimuth:** Angle from MN to the dominating point of the deformation.

**Aperture1:** Angle from MN to first edge of the deformation. If the deformation is located around 0° MN, this angle is noted as a negative angle from MN, e.g. -5°. This angle equals 355°.

**Aperture2:** Angle from MN to last edge of the deformation.

## 6.3 Examples of borehole deformations

### 6.3.1 Example of borehole breakout (BB)

In Figure 6-3 an example of borehole breakout from KFM07C is shown. As there are obvious diametrically opposite deep fallouts, this deformation is classified as BB with the uncertainty as “3” – most certain. As the breakout is seen to be in connection with a fracture crossing the borehole, a “Y” (Yes) is placed in the “Crossing structure” column. Here the deepest and most dominating fallout is seen at 50° and the aperture of the fallout is read to be from 0 to 100°.

The centralization routine is only perfect in a truly circular borehole. Elsewhere it adds some distortion to the centralized images, which can be seen as white (closer) areas around the fallouts. Therefore the most true picture of fallouts is seen on the “Radius”-image and the “Amplitude”-image, as these are not centralized.

### 6.3.2 Example of washout (WO)

In Figure 6-4 an example of washout (WO) from KFM07C is shown. Washouts are separated from breakouts, as there is fallout in the entire perimeter of the borehole, thus the minimum diameter is enlarged. Also here (if possible) a dominating azimuth and aperture angles are read and registered in the Excel sheet.

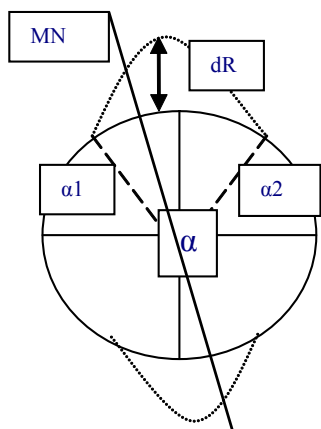
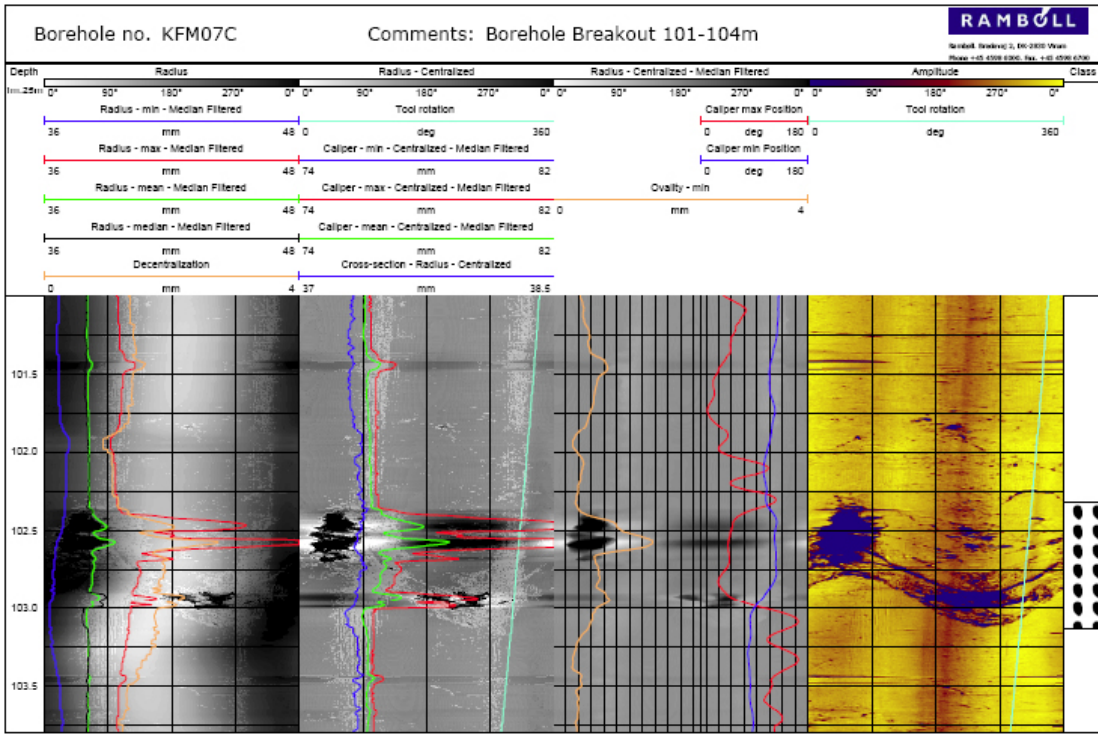
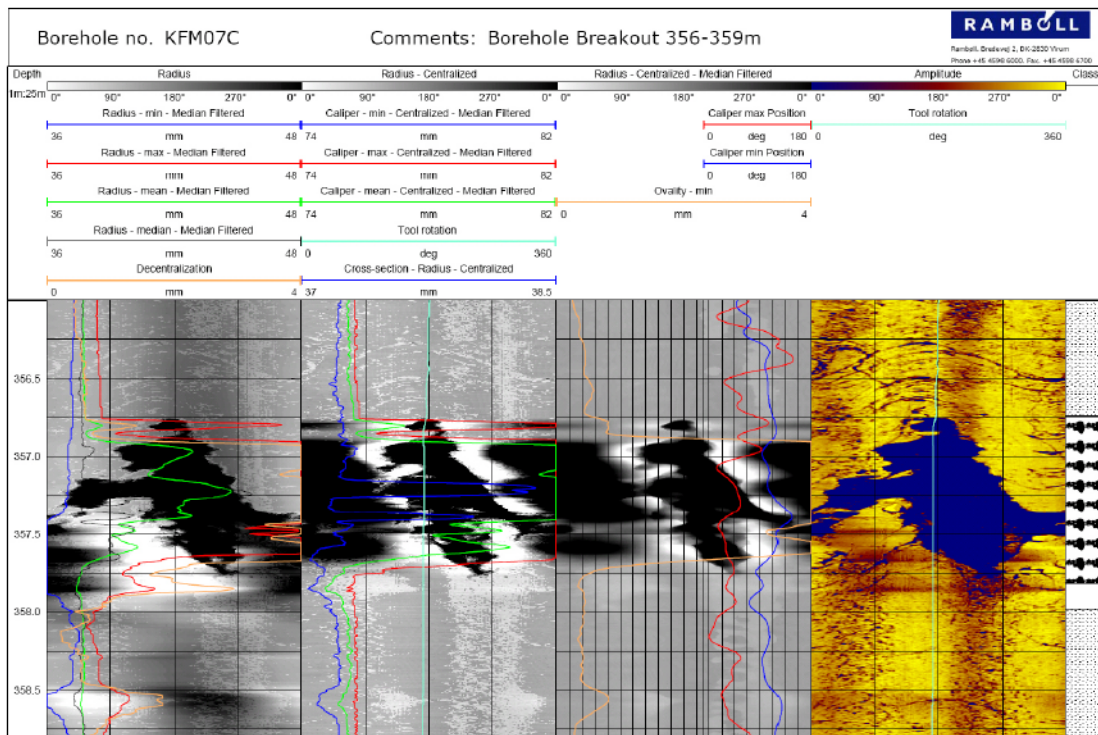


Figure 6-2. Illustration of angles.



**Figure 6-3.** Example of borehole breakout from KFM07C.



**Figure 6-4.** Example of washout from KFM07C.

### 6.3.3 Example of keyseat (KS)

In Figure 6-5 an example of a keyseat (KS) from KFM07C is displayed. The keyseat recognised as a fallout in only one direction at the relevant depth. Also here azimuth and aperture angles are read and registered in the Excel sheet.

### 6.3.4 Example of micro fallout (MF)

In Figure 6-6 an example of micro fallout is presented. In this example the micro fallout is recognized as two vertical bands in the borehole (which here ends in 205m). In these cases azimuth and aperture angles are registered. In other cases the fallout is found in the entire circumference of the borehole (with or without a dominating azimuth). In these cases the aperture angles are registered as 0 to 360°.

The micro fallout is mainly recognised on the Amplitude-image. It is sometimes hard to separate from breakouts, but a condition has been set up, that breakouts should be found also on the Radius-images as darker areas – holes. The registration of micro fallout is generally the most uncertain.

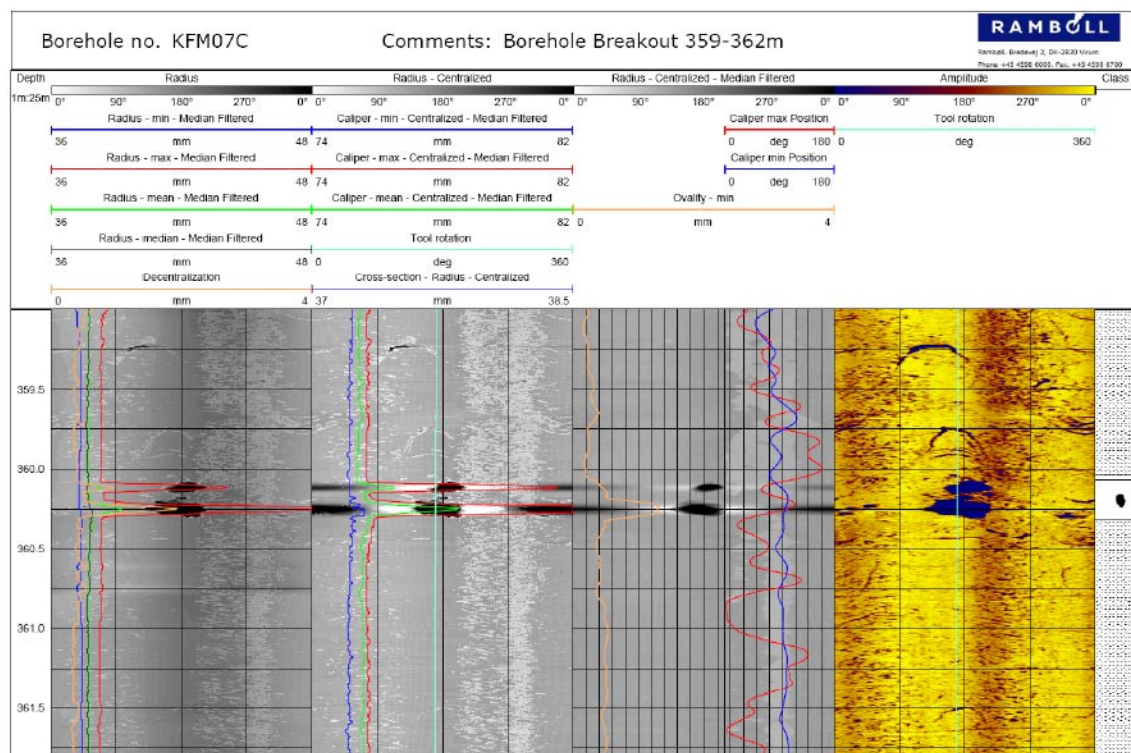


*Figure 6-5. Example of keyseat from KFM07C.*

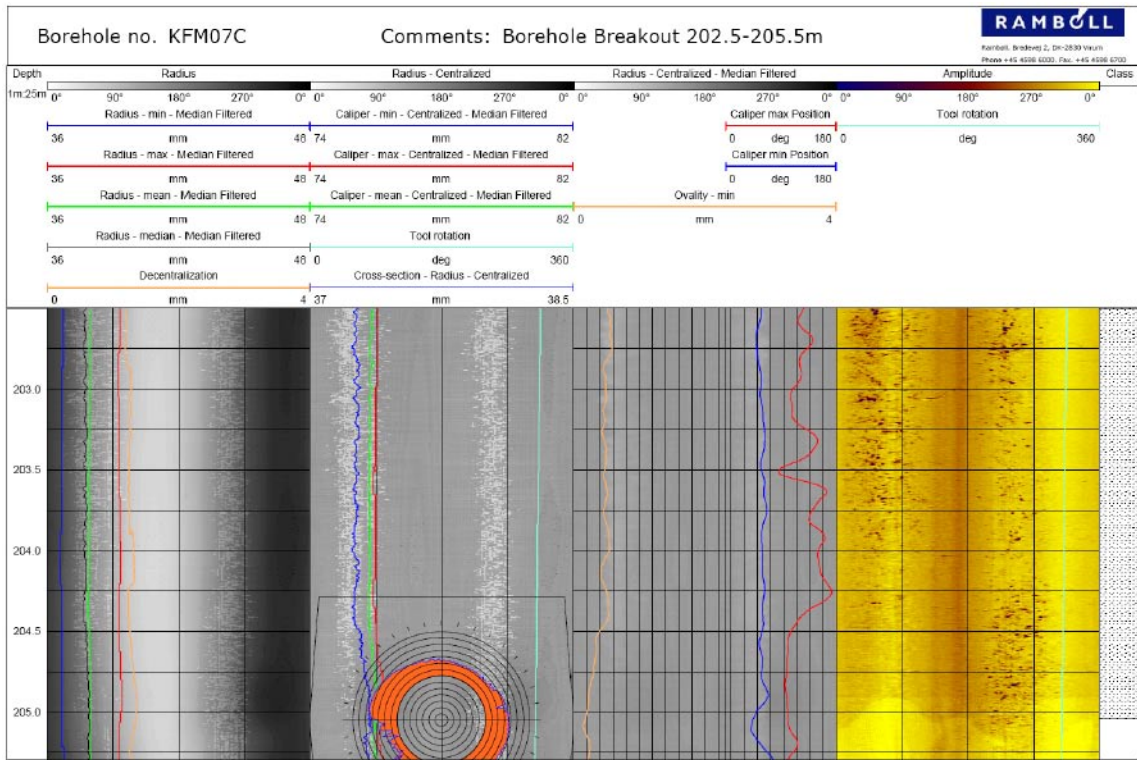


**Figure 6-6.** Example of micro fallout from KFM07C.

## 6.4 Explanation of special features in the borehole

### 6.4.1 Tracks from decentralization

In Figure 6-7 a section from KFM01B with different kinds of tracks and shadows found in the boreholes is shown.

- On the Amplitude image dark tracks are seen which follow the rotation of the tool. These tracks have an internal spacing of  $90^\circ$  and come from the centralizers on the acoustic televiewer probe. This is confirmed by the downrun log, on which they not are present.
- The rotation introduces a slight decentralization of the tool, which also follows the rotation. The remedy of the decentralization is explained in the sections regarding processing, but it still leaves some darker bands on the images. These darker bands, which follow the tool rotation, are artificial.
- Furthermore some vertical tracks are observed on both the amplitude- and radius-images. They are anticipated to have been made by centralizers from other probes, e.g. the BIPS-probe. In parts of the borehole, they are also recognised on the BIPS-image. /Gustafson and Gustafson 2004/.

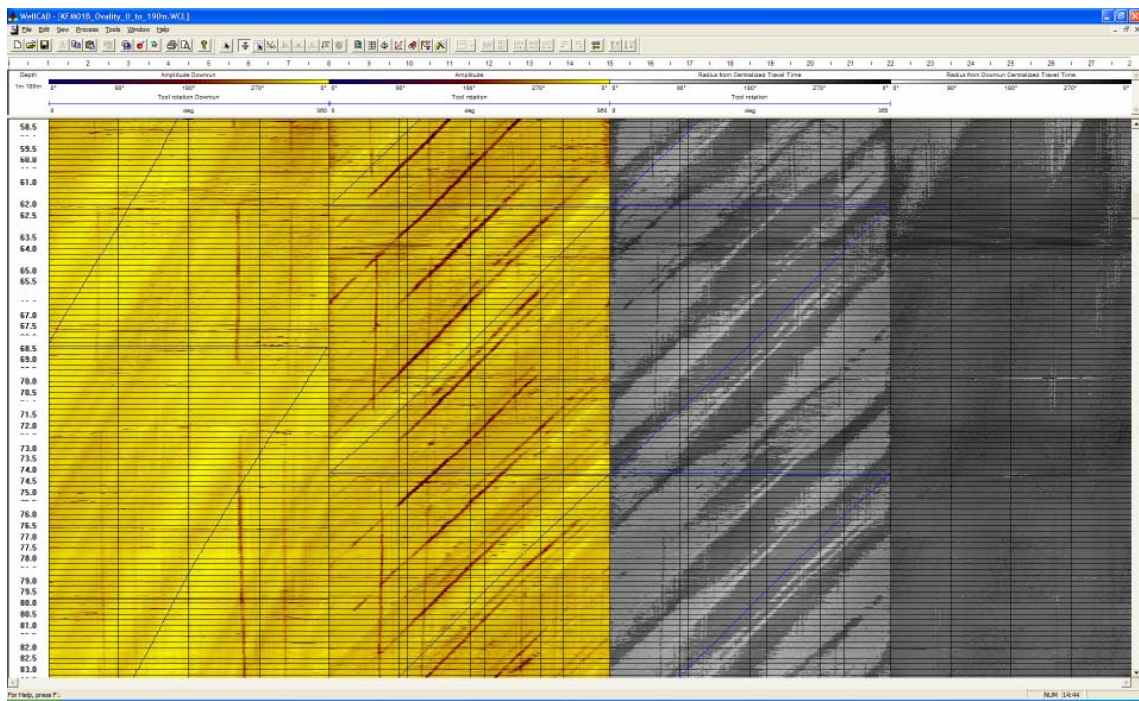


**Figure 6-7.** Tracks and shadows in KFM01B, 58.5 to 83 m.

#### 6.4.2 Drill cuttings from bottom of borehole

In Figure 6-8 an example from the bottom of KFM01B is presented. Here drilling debris from the bottom of the hole has partly covered the acoustic window, but is slowly washed off.

#### 6.4.3 Wobbles from drilling process

In Figure 6-9 an example of “wobbles” made by the drilling process is displayed. These wobbles are frequently seen in the boreholes and in some cases they make it hard to register deformations in these areas. In KFM03A they are registered in a separate table.

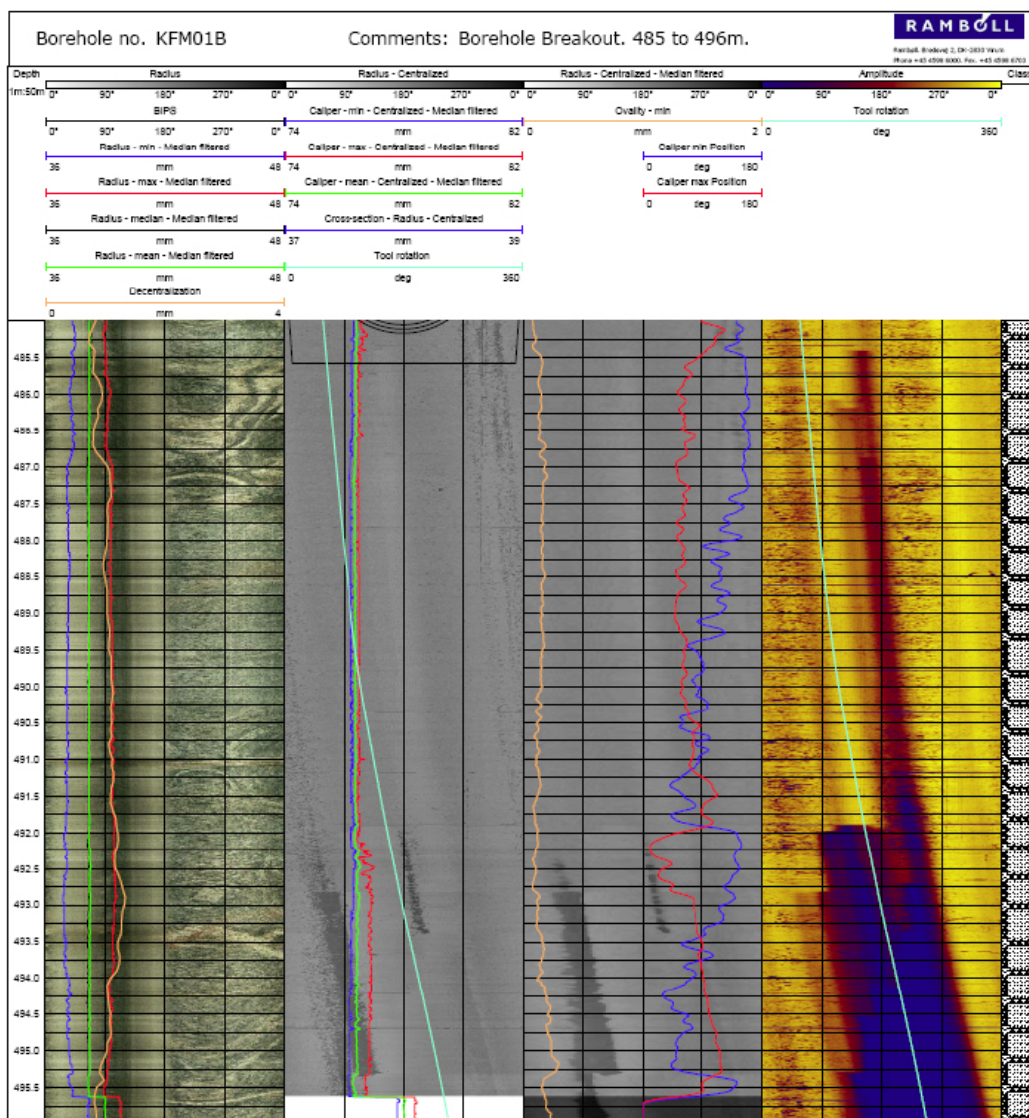


**Figure 6-8.** Example of drill cuttings on the acoustic window.

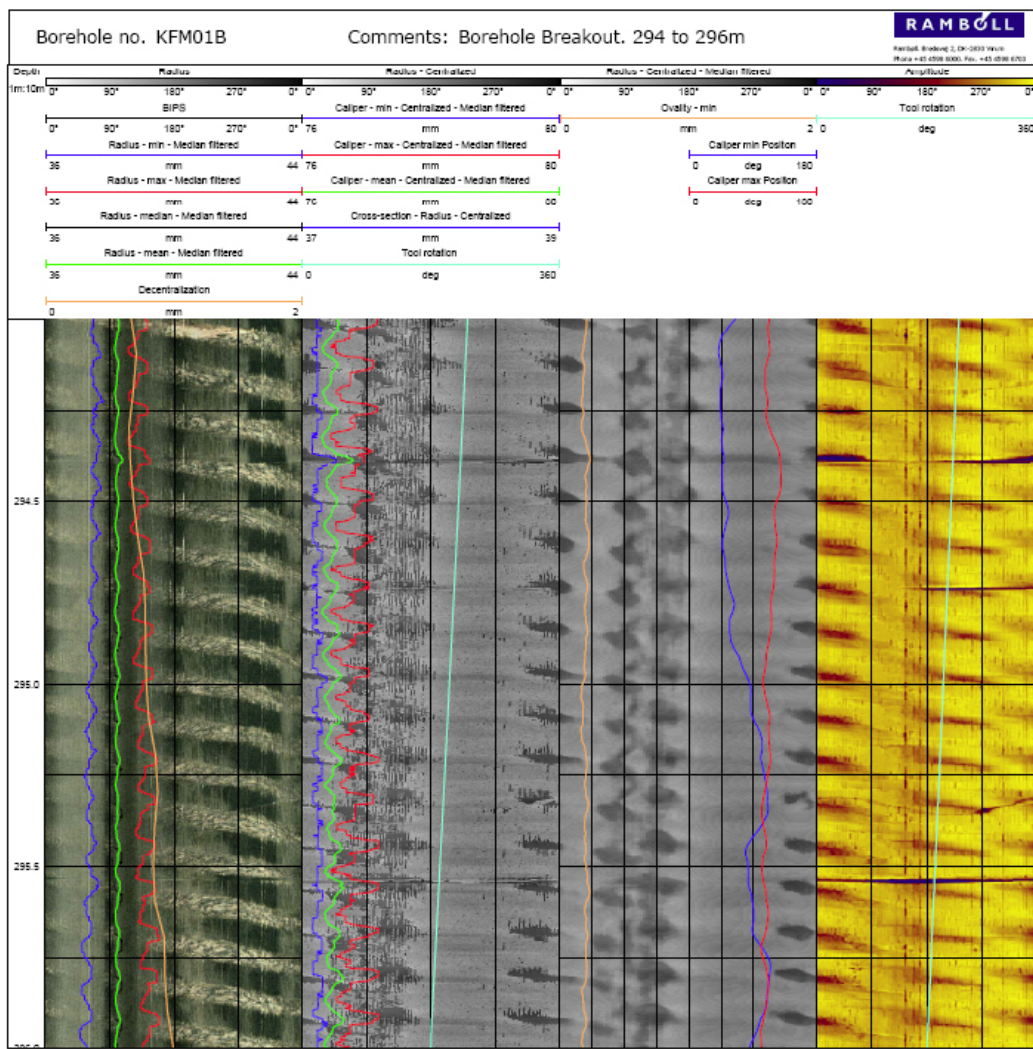


Figure 6-9. Example of wobbles.

## 7 Summary and discussions

- It is relatively fast to locate larger deformations, simply by means of scrolling through a calculated high resolution caliper.
- Orientation and size of the deformations can be precisely mapped.
- There is an obvious tendency that the main azimuth of breakouts and micro fallouts in all the boreholes is found to be at 40 to 60° from magnetic north.
- In KFM07C deformations covering about 2/3 of the borehole length were registered.
- The cross-sections are often too disturbed of noise from decentralization to be used.
- It is strongly recommended, that the logpanels are evaluated in WellCAD or the free WellCAD-reader, as a print-out or PDF does not provide the necessary flexibility to zoom and focus on relevant deformations.
- No ovality in the boreholes exceeding 0.1 mm has been found, unless it is related to fallouts or breakouts.
- In KFM01B there are lots of fractures, which can be recognised on the acoustic televiewer images, but not found on the BIPS-image. If these fractures are of interest, they could be picked on televiewer images. Examples from KFM01B: 353.85 m, 354.23 m, 356.12 m, 356.21 m, 356.88 m, 357.18 m, 357.71 m, etc. This tendency is anticipated to be valid for all boreholes
- One or more of the boreholes could be logged and processed again. As the first boreholes were logged more than 3 years ago, it would be relevant to see if there has been a time dependent development in the deformations.
- When smaller breakouts or micro fallout are found in connection with fractures, it can be difficult to clarify, whether the fallout was caused by the drilling process or by stress.

## References

- Ask M V S, Ask D, Christiansson R, 2006.** Detection of borehole breakouts at the Forsmark site, Sweden. Proc. Int. Symp. on In-Situ Rock Stress (Eds. Lu M, Li CC, Kjørholt H, Dahle H), June 19–21, 2006, Trondheim, Norway, pp. 79–86.
- Ask D, Ask M V S, 2007.** Detection of potential borehole breakouts in boreholes KFM01A and KFM01B. SKB P-report in prep. Svensk Kärnbränslehantering AB.
- Deltombe J-L, Schepers R, 2000.** Combined Processing of BHTV Traveltime and Amplitude Images. In Proc. Int. Symp. Borehole Geophysics for Minerals, Geotechnical, and Groundwater applications, Golden, CO, United States, Vol. 7 pp. 29–42.
- Gustafsson J, Gustafsson C, 2004.** RAMAC- and BIPS-logging in borehole KFM01B and RAMAC directional re-logging in borehole KFM01A. SKB P-04-79. Svensk Kärnbränslehantering AB.
- Plumb R A, Hickman SH, 1985.** Stress-induced borehole elongation: A comparison between four-arm dipmeter and the borehole televiewer in the Auburn geothermal well. *J. Geophys. Res.*, 90, pp. 5513–21.
- Siddans A W B, Worthington P, 2003.** Structural geology using borehole wall imagery. Case studies of 3 HiRAT logs. Not published, can be found on Robertson Geologgings homepage.
- Zoback M D, Moos D, Martin L, Andersson R N, 1985.** Borehole breakouts and in situ stress. *J. Geophys. Res.*, 90, pp. 5523–30.

## **Appendix A**

### **List of acquisition reports**

List of acquisition reports from logging with acoustic televiewer, fluid temperature and resistivity – and calculation of fluid velocity.

- KFM01A: SKB P-03-103. Geophysical borehole logging in borehole KFM01A, HFM01 and HFM02. Forsmark site investigation. Nielsen, Uffe Torben; Ringgaard, Jørgen. 2004.
- KFM01B: SKB P-04-145. Geophysical borehole logging in borehole KFM01B, HFM14, HFM15, HFM16, HFM17 and HFM18. Forsmark site investigation. Nielsen, Uffe Torben; Ringgaard, Jørgen. 2004.
- KFM02A, KFM03A, KFM03B: SKB P-04-97. Geophysical borehole logging in borehole KFM02A, KFM03A and KFM03B. Forsmark site investigation. Nielsen, Uffe Torben; Ringgaard, Jørgen. 2004.
- KFM04A: SKB P-04-144. Geophysical borehole logging in borehole KFM04A, KFM06A, HFM10, HFM11, HFM12 and HFM13. Forsmark site investigation. Nielsen, Uffe Torben; Ringgaard, Jørgen. 2004.
- KFM05A: SKB P-04-153. Geophysical borehole logging in borehole KFM05A and HFM19. Forsmark site investigation. Nielsen, Uffe Torben; Ringgaard, Jørgen. 2004.
- KFM06A: SKB P-05-17. Geophysical borehole logging in borehole KFM06A, HFM20, HFM21, HFM22 and SP-logging in KFM01A and KFM04A. Forsmark site investigation. Nielsen, Uffe Torben; Ringgaard, Jørgen; Horn, Frederik. 2005.
- KFM07C: SKB P-07-04. Geophysical borehole logging in boreholes KFM07C, HFM36 and HFM37. Forsmark site investigation. Nielsen, Uffe Torben; Ringgaard, Jørgen, 2007.



## Appendix B

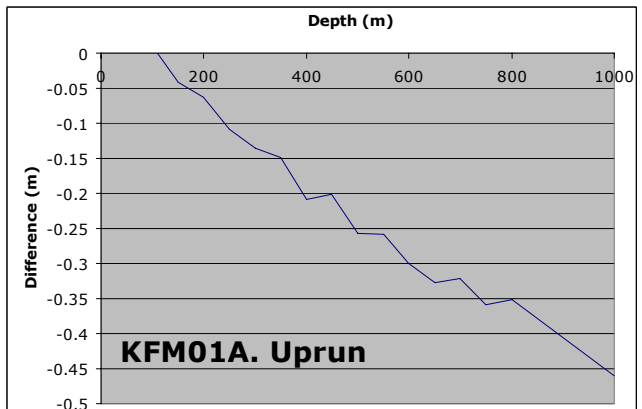
### Tables and charts of depth errors

#### KFM01A

##### **KFM01A. Uprun**

True depth	HiRAT	Difference
110	110	0
150	150.041	-0.041
200	200.063	-0.063
250	250.109	-0.109
300	300.136	-0.136
350	350.149	-0.149
400	400.209	-0.209
450	450.202	-0.202
500	500.257	-0.257
550	550.258	-0.258
600	600.3	-0.3
650	650.327	-0.327
700	700.322	-0.322
750	750.359	-0.359
800	800.352	-0.352
1000.5	1000.96	-0.46

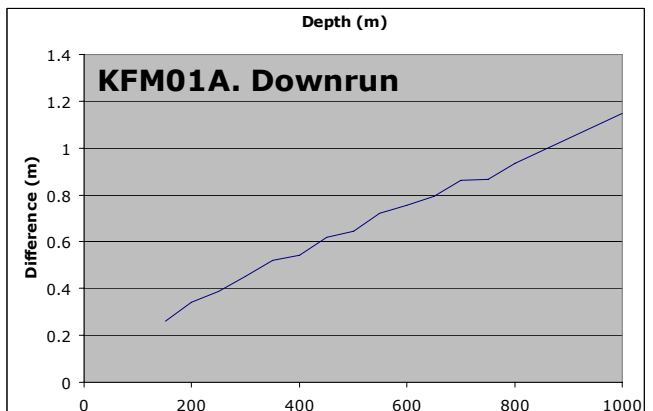
The bottom is derived - linearity anticipated



##### **KFM01A. Downrun**

True depth	HiRAT	Difference
150	149.74	0.26
200	199.66	0.34
250	249.61	0.39
300	299.547	0.453
350	349.48	0.52
400	399.46	0.54
450	449.38	0.62
500	499.356	0.644
550	549.278	0.722
600	599.246	0.754
650	649.206	0.794
700	699.138	0.862
750	749.132	0.868
800	799.067	0.933
1000.5	999.35	1.15

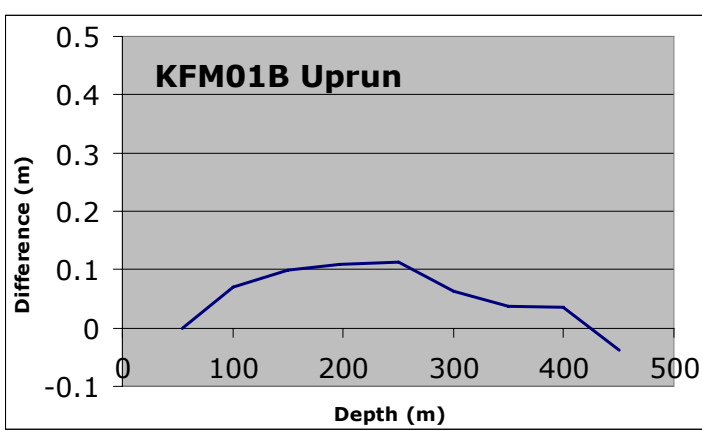
The bottom is derived - linearity anticipated



## KFM01B

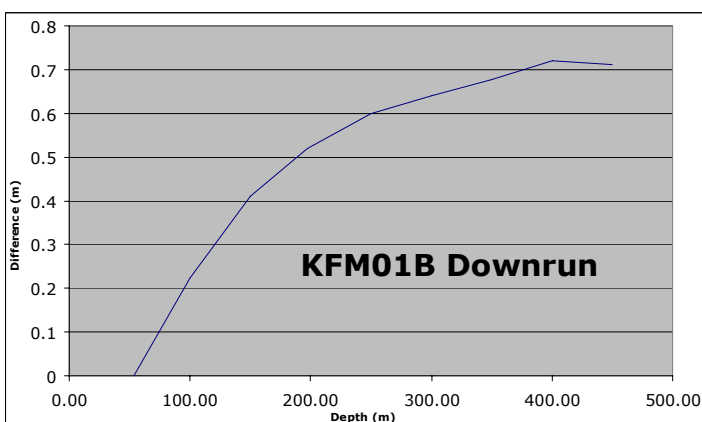
### KFM01B. Uprun

True depth	HiRAT	Difference
54.00	54	0
100.00	99.931	0.069
150.00	149.901	0.099
197.00	196.891	0.109
250.00	249.887	0.113
300.00	299.938	0.062
350.00	349.963	0.037
400.00	399.964	0.036
450.00	450.038	-0.038



### KFM01B. Downrun

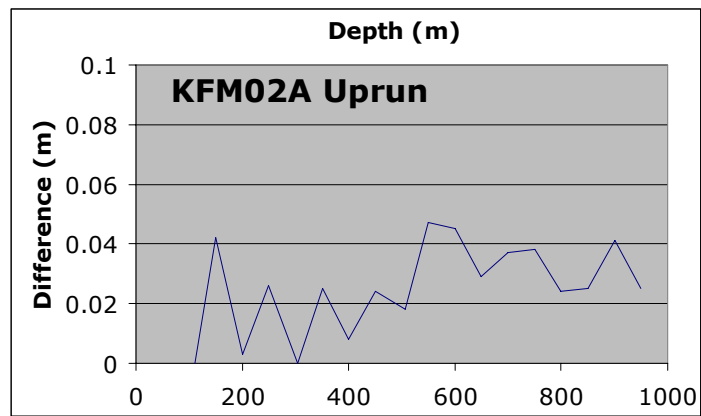
True depth	HiRAT	Difference
54.00	54	0
100.00	99.776	0.224
150.00	149.59	0.41
197.00	196.481	0.519
250.00	249.4	0.6
300.00	299.36	0.64
350.00	349.323	0.677
400.00	399.28	0.72
450.00	449.29	0.71



## KFM02A

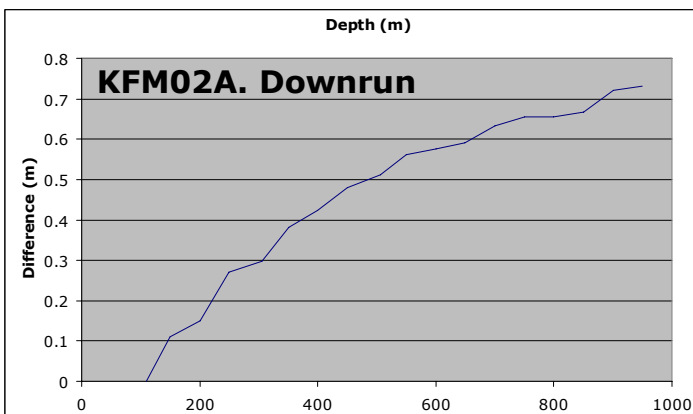
### KFM02A. Uprun

True depth	HiRAT	Difference
110	110	0
150	149.958	0.042
200	199.997	0.003
250	249.974	0.026
304.5	304.5	0
350	349.975	0.025
400	399.992	0.008
450	449.976	0.024
506	505.982	0.018
550	549.953	0.047
600	599.955	0.045
650	649.971	0.029
700	699.963	0.037
750	749.962	0.038
800	799.976	0.024
850	849.975	0.025
900	899.959	0.041
950	949.975	0.025



### KFM02A. Downrun

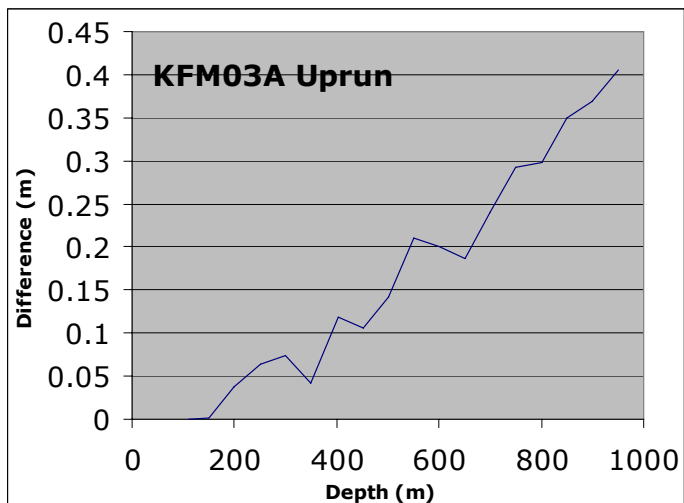
True depth	HiRAT	Difference
110	110	0
150	149.89	0.11
200	199.849	0.151
250	249.729	0.271
304.5	304.201	0.299
350	349.618	0.382
400	399.577	0.423
450	449.521	0.479
506	505.487	0.513
550	549.439	0.561
600	599.423	0.577
650	649.409	0.591
700	699.367	0.633
750	749.345	0.655
800	799.344	0.656
850	849.333	0.667
900	899.279	0.721
950	949.27	0.73



## KFM03A

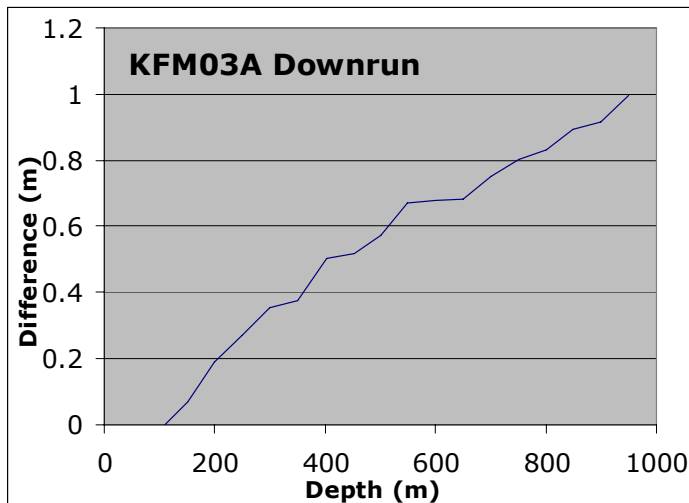
### KFM03A. Uprun

True depth	HiRAT	Difference
110	110	0
150	149.999	0.001
200	199.962	0.038
250	249.936	0.064
300	299.926	0.074
350	349.958	0.042
403	402.882	0.118
453	452.894	0.106
500	499.858	0.142
550	549.789	0.211
600	599.8	0.2
650	649.814	0.186
700	699.759	0.241
750	749.708	0.292
800	799.702	0.298
850	849.65	0.35
900	899.631	0.369
950	949.595	0.405



### KFM03A. Downrun

True depth	HiRAT	Difference
110	110	0
150	149.93	0.07
200	199.81	0.19
250	249.729	0.271
300	299.645	0.355
350	349.625	0.375
403	402.496	0.504
453	452.482	0.518
500	499.427	0.573
550	549.33	0.67
600	599.323	0.677
650	649.319	0.681
700	699.248	0.752
750	749.199	0.801
800	799.168	0.832
850	849.107	0.893
900	899.083	0.917
950	949.005	0.995

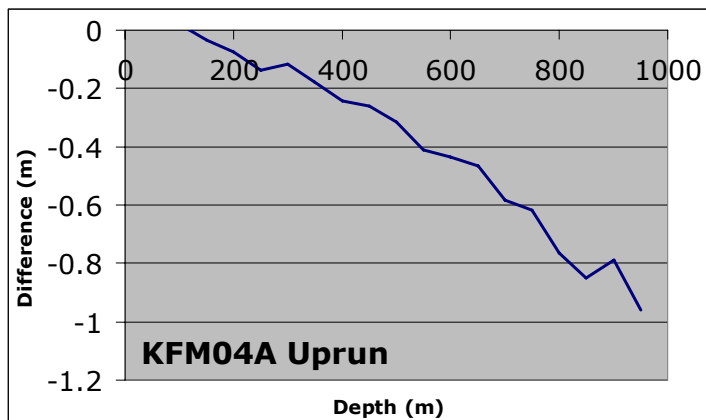


## KFM04A

There was an error in the file from 730 to 900 m. A manual stretch has been performed with a reasonable result. The plot is made before the manuel stretch was applied.

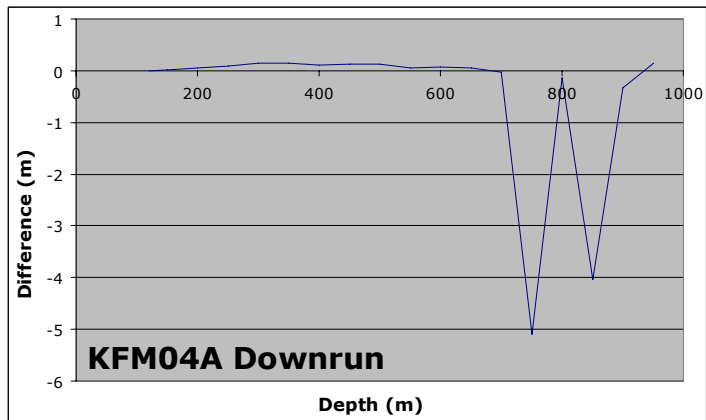
### KFM04A. Uprun

True depth	HiRAT	Difference
108.61	108.6	0.01
119.00	119	0
150.00	150.033	-0.033
200.00	200.075	-0.075
250.00	250.137	-0.137
300.00	300.117	-0.117
350.00	350.177	-0.177
400.00	400.245	-0.245
450.00	450.26	-0.26
500.00	500.316	-0.316
550.00	550.41	-0.41
600.00	600.437	-0.437
650.00	650.467	-0.467
700.00	700.583	-0.583
750.00	750.617	-0.617
800.00	800.764	-0.764
850.00	850.851	-0.851
900.00	900.789	-0.789
950.00	950.961	-0.961



### KFM04A. Downrun

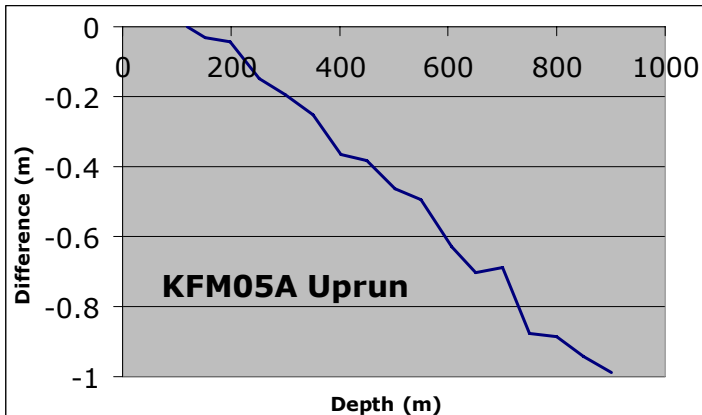
True depth	HiRAT	Difference
119.00	119	0
150.00	149.983	0.017
200.00	199.941	0.059
250.00	249.91	0.09
300.00	299.84	0.16
350.00	349.85	0.15
400.00	399.88	0.12
450.00	449.87	0.13
500.00	499.87	0.13
550.00	549.94	0.06
600.00	599.92	0.08
650.00	649.94	0.06
700.00	700.022	-0.022
750.00	755.1	-5.1
800.00	800.13	-0.13
850.00	854.03	-4.03
900.00	900.34	-0.34
950.00	949.84	0.16



## KFM05A

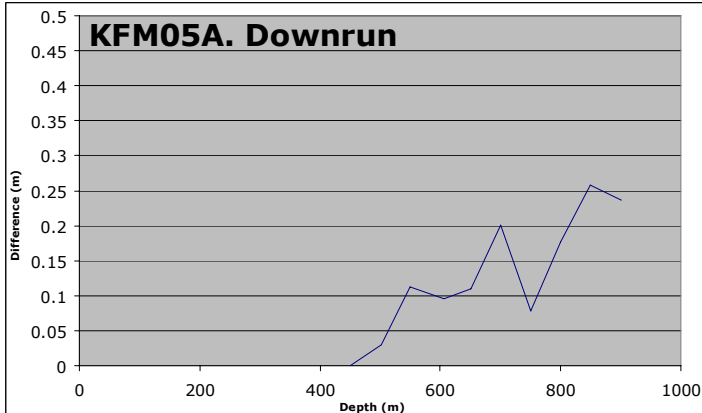
### KFM05A. Uprun

True depth	HiRAT	Difference
120.00	120	0
152.00	152.032	-0.032
199.00	199.044	-0.044
252.00	252.148	-0.148
300.00	300.194	-0.194
352.00	352.251	-0.251
402.00	402.366	-0.366
450.00	450.382	-0.382
501.00	501.463	-0.463
550.00	550.495	-0.495
606.00	606.63	-0.63
650.00	650.702	-0.702
700.00	700.689	-0.689
750.00	750.877	-0.877
800.00	800.887	-0.887
850.00	850.942	-0.942
900.00	900.988	-0.988



### KFM05A. Downrun

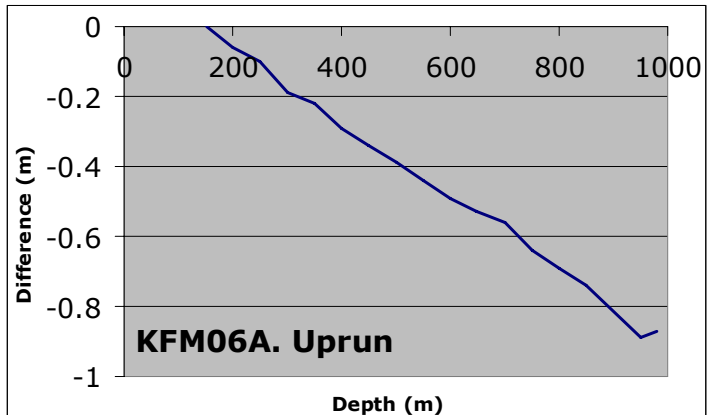
True depth	HiRAT	Difference
450.00	450	0
501.00	500.97	0.03
550.00	549.888	0.112
606.00	605.905	0.095
650.00	649.891	0.109
700.00	699.799	0.201
750.00	749.921	0.079
800.00	799.824	0.176
850.00	849.742	0.258
900.00	899.764	0.236



## KFM06A

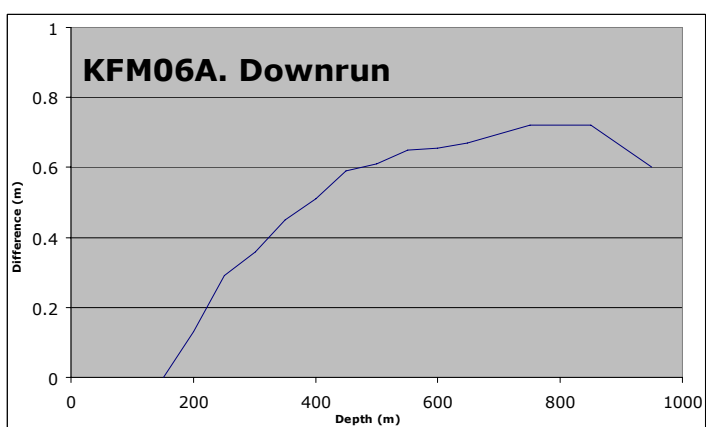
### KFM06A. Uprun

True depth	HiRAT	Difference
152.00	152	0
200.00	200.06	-0.06
250.00	250.1	-0.1
301.00	301.19	-0.19
350.00	350.22	-0.22
400.00	400.29	-0.29
450.00	450.34	-0.34
500.00	500.39	-0.39
550.00	550.44	-0.44
600.00	600.49	-0.49
648.00	648.53	-0.53
700.00	700.56	-0.56
750.00	750.64	-0.64
800.00	800.69	-0.69
850.00	850.74	-0.74
950.00	950.89	-0.89
980	980.87	-0.87



### KFM06A. Downrun

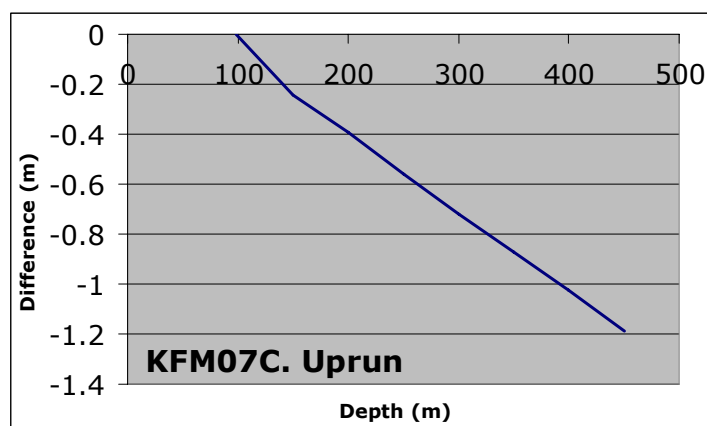
True depth	HiRAT	Difference
152.00	152	0
200.00	199.87	0.13
250.00	249.71	0.29
301.00	300.64	0.36
350.00	349.55	0.45
400.00	399.49	0.51
450.00	449.41	0.59
500.00	499.39	0.61
550.00	549.35	0.65
600.00	599.344	0.656
648.00	647.33	0.67
750.00	749.28	0.72
850.00	849.28	0.72
950.00	949.4	0.6



## KFM07C

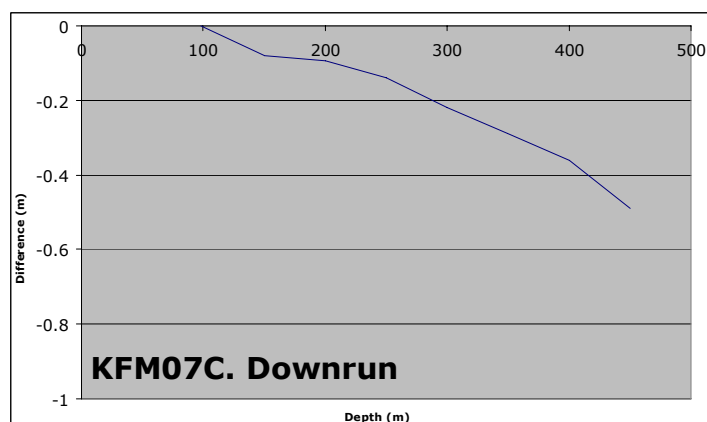
### KFM07C. Uprun

True depth	HiRAT	Difference
98.39	98.39	0
150.00	150.245	-0.245
200.00	200.392	-0.392
250.00	250.559	-0.559
300.00	300.718	-0.718
350.00	350.873	-0.873
400.00	401.024	-1.024
450.00	451.189	-1.189



### KFM07C. Downrun

True depth	HiRAT	Difference
98.39	98.39	0
150.00	150.08	-0.08
200.00	200.093	-0.093
250.00	250.14	-0.14
300.00	300.22	-0.22
350.00	350.29	-0.29
400.00	400.36	-0.36
450.00	450.49	-0.49

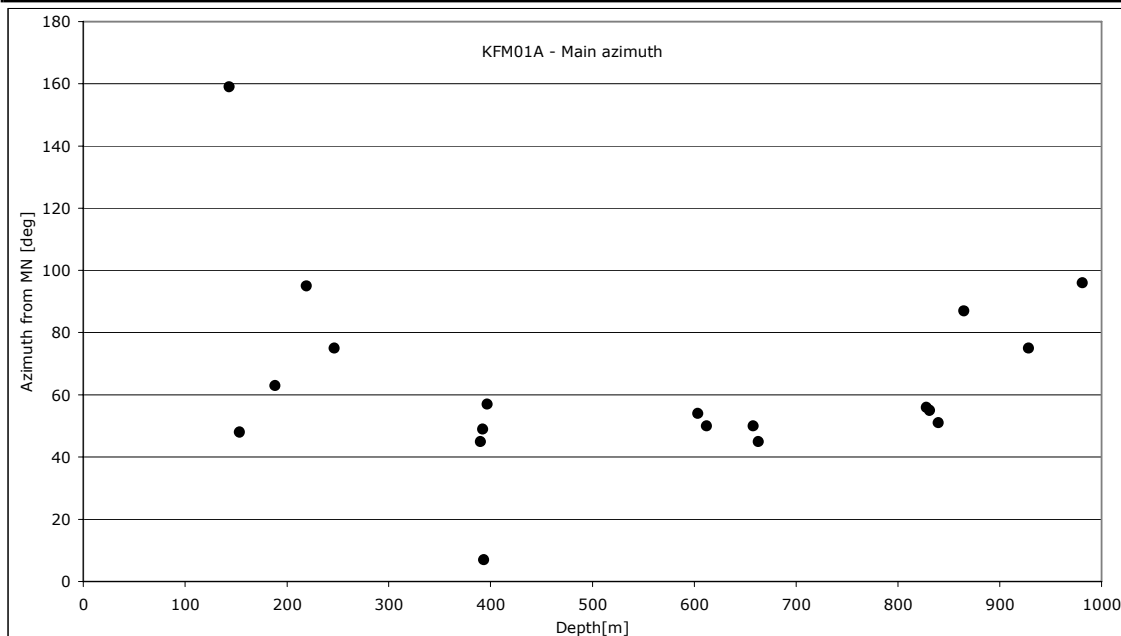


## Appendix C

### Tables and charts of registered deformations.

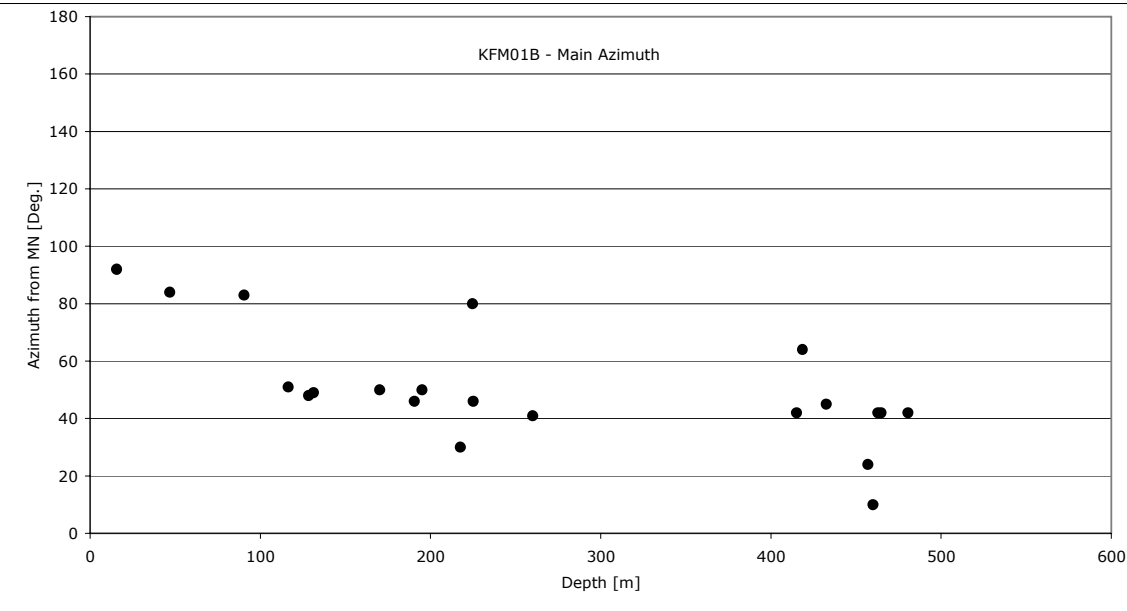
#### KFM01A

KFM01A - Observed BB, WO, KS and MF												
Top Dept	Bot. dept	Max R	Median R	dRmax	Class	Cross. struc	Uncertainty	Main Azimuth	Azimuth	Aperture a1	Aperture a2	Comments
[m]	[m]	[mm]	[mm]	[mm]		[0-3]	[Y/Yes/No]	[° from MN]	[° from MN]	[° from MN]	[° from MN]	
136.3	149.6	38.7	38.6	0.1	MF	N	1			0	360	
143.3	145.1	44.0	38.6	5.5	BB	N	1	159	159	108	213	
153.5	153.69	38.8	38.3	0.5	BB	Y	2	48	48	39	63	
170	188	38.7	38.6	0.1	MF		1					
188.23	188.36	39.1	38.6	0.6	BB	Y	3	63	63	51	76	
190.7	191	40.6	38.4	2.2	WO	N	1					
219.1	219.6	40.5	38.4	2.1	KS	N	2	95	95	84	210	
246.5	247.4	39.1	38.7	0.4	BB	Y	2	75	255	225	219	
262	292	38.4	38.3	0.1	MF		1					
368	383	38.4	38.3	0.1	MF		1					
390	396	38.4	38.3	0.1	MF	Y	1	45	45			
392.1	392.28	41.7	38.2	3.4	KS	N	2	49	49	49	-5	
393.35	393.44	39.3	38.2	1.0	KS	N	2	7	187	7	331	
396.73	397.1	67.0	38.2	28.8	WO	Y	2	57	237	237	69	
397.5	409.5	38.4	38.3	0.1	MF		2					
428.5	491	38.4	38.3	0.1	MF		1					
510	540.8	38.4	38.3	0.1	MF		1					
573	606	38.4	38.3	0.1	MF		1					
603.35	603.58	40.5	38.3	2.2	BB	Y	3	54	234	201	261	
612.06	612.85	39.0	38.5	0.5	BB	N	3	50	50	15	80	
657.84	658.25	40.5	38.4	2.1	BB	Y	3	50	230	200	270	
662.95	669.8	40.5	38.5	2.0	BB	Y	2	45	45	21	66	A few small BB
670.9	674.73	41.0	38.5	2.5	WO	Y	2					
716.7	717	39.5	38.4	1.1	WO	N	1					
828	828.79	39.0	38.5	0.5	BB	Y	2	56	56	40	75	
831	832.7	39.0	38.5	0.5	BB	N	3	55	55	30	90	
839.75	843.65	38.8	38.5	0.3	BB	Y	3	51	231	204	270	
864.7	864.95	38.7	38.5	0.2	BB	Y	3	87	87	57	11	
888	945.5	38.6	38.5	0.1	MF	N	1					
928.2	928.5	44.0	38.5	5.5	BB	N	3	75	75	27	138	
981.1	981.25	43.0	38.5	4.5	BB	N	3	96	96	40	156	



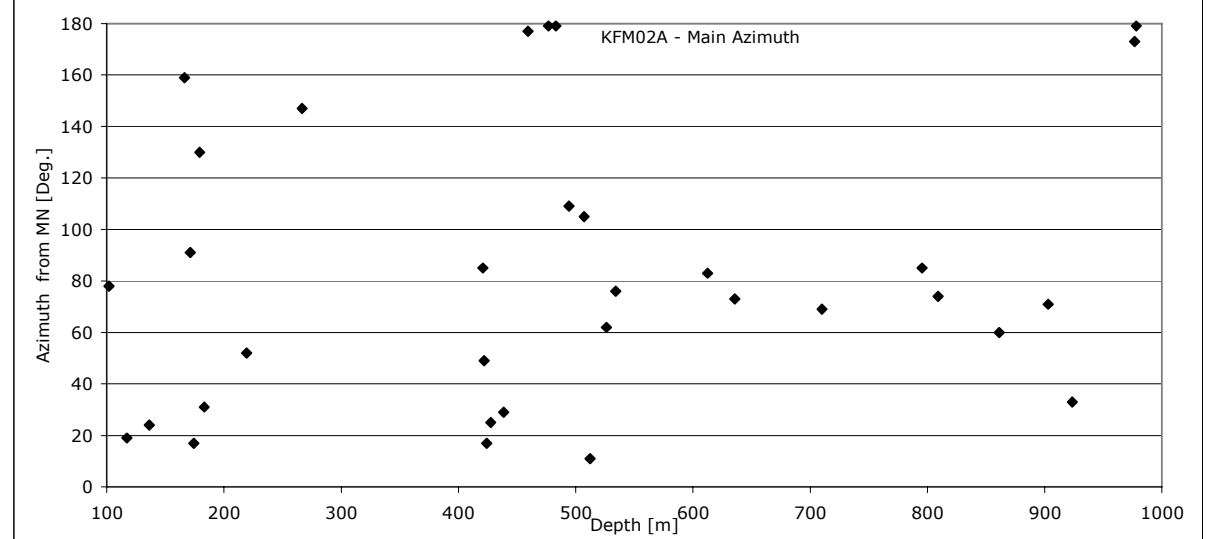
## KFM01B

KFM01B - Observed BB, WO, KS and MF													
Top	Depth	Bot. depth	Max R	Median R	dRmax	Class	Uncertainty	Cross. struct.	Main Azimuth	Azimuth	Aperture α1	Aperture α2	Comments
[m]	[m]	[mm]	[mm]	[mm]			[0-3]	[Yes/No]	[° from MN]	[° from MN]	[° from MN]	[° from MN]	
15.50	65.00	39.0	38.6	0.4		KS	3	N	92	272	260	284	
39.75	41.85	38.8	38.7	0.1		MF	2	Y			0	360	
46.80	48.40	40.7	38.5	2.2		BB	2	Y	84	264	217	287	
48.96	50.64	38.7	38.6	0.1		MF	2	Y			0	360	
90.44	90.84	39.2	38.5	0.7		BB	2	Y	83	83	57	109	
116.40	117.26	38.5	38.4	0.1		MF	3	Y	51	51	0	100	
128.40	129.73	38.4	38.3	0.1		MF	3	Y	48	48	0	100	
131.25	132.44	41.9	38.2	3.8		KS	2	N	49	229	192	262	
170.00	188.43	38.3	38.2	0.1		MF	3	Y	50	230	180	280	
190.50	200.00	38.3	38.2	0.1		MF	3	Y	46	226	190	270	
195.00	203.00	39.0	38.2	0.8		BB	2	Y	50	50	30	70	3 small BB
217.47	217.60	41.1	38.2	2.9		BB	3	N	30	210	198	228	
224.72	224.81	39.2	38.2	1.0		BB	2	Y	80	80	0	154	
225.00	234.70	38.3	38.2	0.1		MF	2	Y	46	226	192	265	
260.00	262.40	38.3	38.2	0.1		MF	2	Y	41	41	0	85	
415.00	470.06	38.3	38.2	0.1		MF	3	Y	42	42	0	360	
418.50	419.30	50.0	38.2	11.8		WO	2	Y	64	244			
432.50	444.90	50.0	38.2	11.8		BB	3	Y	45	45	-10	96	Several BB
456.90	457.20	43.0	38.3	4.7		BB	2	Y	24	24	-30	60	
462.95	463.39	42.1	38.3	3.8		BB	3	N	42	42	0	85	
464.75	464.90	43.2	38.3	4.9		BB	3	N	42	42	0	85	
460.00	480.00	39.5	38.3	1.3		KS	2	N	10	190	180	200	
480.60	498.00	38.4	38.3	0.1		MF	3	Y	42	42	0	100	



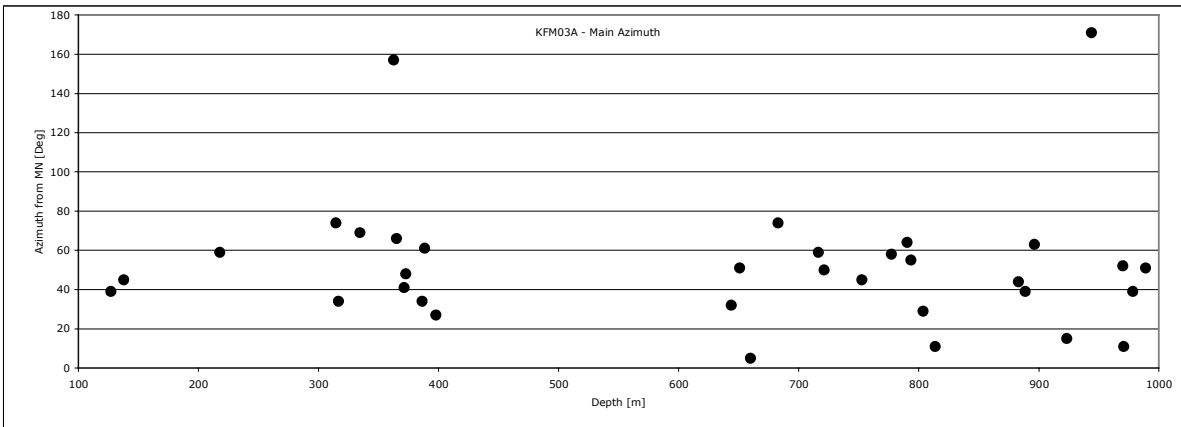
## KFM02A

KFM02A - Observed BB, WO, MF and KS													
Top Depth	Bot. depth	Max R	Median R	dRmax	Structure	Uncertainty	Cross. struct.	Main Azimuth	Azimuth	Aperture a1	Aperture a2	Comments	
[m]	[m]	[mm]	[mm]	[mm]		[0-3]	[Yes/No]	[° from MN]	[° from MN]	[° from MN]	[° from MN]		
102	106.39	38.5	38.4	0.1	MF	2	N	78	258	0	360		
117.24	120.00	65.0	38.8	26.2	WO	2	Y	19	19	69	69		
136.20	137.12	39.5	38.8	0.7	BB	2	N	24	204	159	249		
166.30	166.57	41.0	38.9	2.1	BB	1	N	159	159	93	209		
171.26	172.03	95.0	38.9	56.1	BB	1	N	91	271	189	321		
174.30	174.63	41.4	38.8	2.6	BB	1	Y	17	197	171	249		
179.37	180.04	39.0	38.9	0.1	MF	3	N	130	130	0	360		
183.12	183.27	48.9	38.8	10.1	KS	1	N	31	211	203	247		
219.17	219.65	39.7	38.8	0.9	BB	2	Y	52	52	20	82		
248.00	297.00	39.9	38.8	1.1	MF	3	N			0	360		
266.57	267.23	108.7	38.8	69.9	WO	2	Y	147	147	95	197		
298.87	299.51	40.4	38.9	1.5	MF	3	N			0	360		
420.69	421.36	39.0	38.9	0.1	MF	3	N	85	85	56	106		
421.85	422.94	46.8	38.9	7.9	BB	2	Y	49	49	-21	93		
424.04	424.19	42.1	38.9	3.2	BB	2	Y	17	17	355	39		
427.60	427.71	43.1	38.9	4.2	BB	3	N	25	205	143	255		
438.47	440.38	40.5	39.9	0.6	BB	2	Y	29	209	197	223		
459.31	459.54	46.1	39.9	6.2	BB	3	N	177	177	145	205		
476.73	477.23	45.2	38.9	6.3	BB	1	Y	179	179	117	237		
483.12	483.60	45.9	39.0	7.0	BB	3	Y	179	179	141	217		
494.16	498.35	68.3	38.9	29.4	BB	3	Y	109	109	69	133		
507.26	507.32	45.0	39.0	6.1	BB	3	N	105	285	255	313		
512.26	513.83	89.7	38.9	50.8	BB	2	Y	11	191	127	201		
526.30	238.29	38.9	38.8	0.1	MF	2	N	62	62	0	90		
534.16	538.28	38.8	38.7	0.1	MF	2	N	76	76	48	110		
612.59	612.81	41.7	38.6	3.1	BB	2	N	83	263	237	301		
635.60	638.00	40.0	38.8	1.2	BB	1	Y	73	253	229	279		
710.00	747.15	42.0	38.6	3.4	BB	1	Y	69	249	239	259	Six small BB	
795.30	795.79	43.0	38.7	4.3	BB	3	N	85	265	213	301		
809.06	817.66	39.0	38.6	0.4	MF	2	N	74	74	0	360		
861.30	872.90	39.0	38.8	0.2	MF	2	N	60	60	0	100		
902.90	903.33	46.4	39.0	7.4	BB	3	Y	71	251	231	295		
923.64	925.08	41.7	38.9	2.8	BB	3	Y	33	213	159	245		
976.70	979.00	42.7	38.9	3.8	KS	2	N	173	173	169	181		
978.30	979.30	47.4	39.0	8.3	WO	2	Y	179	179	69	69		

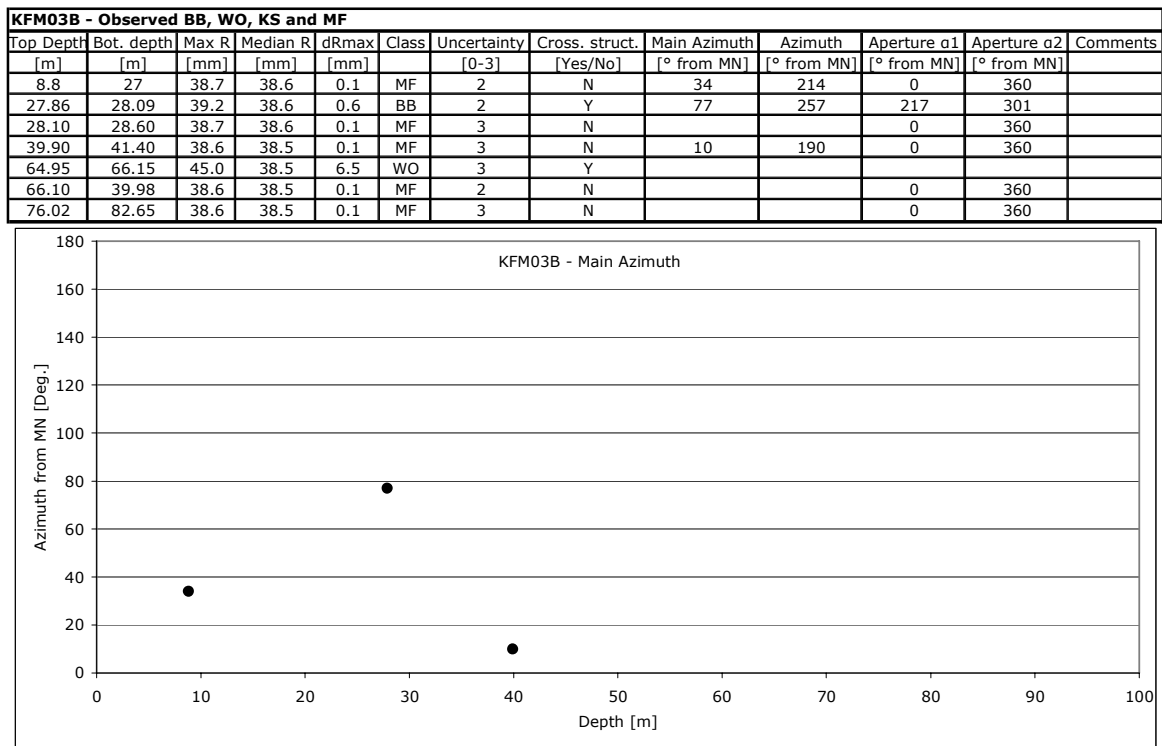


## KFM03A

KFM03A - Observed BB, WO, KS and MF													
Top Depth [m]	Bot. depth [m]	Max R [mm]	Median R [mm]	dRmax [mm]	Structure	Uncertainty [0-3]	Cross. struct.	Main Azimuth [° from MN]	Azimuth [° from MN]	Aperture a1 [° from MN]	Aperture a2 [° from MN]	Comments	
127.16	127.50	40.2	38.6	1.6	BB	2	N	39	219	165	249		
137.95	139.20	38.7	38.6	0.1	MF	3	Y	45	45	0	90		
217.85	218.58	39.8	38.7	1.1	BB	2	Y	59	239	223	257		
314.60	314.70	41.0	38.8	2.2	BB	2	Y	74	74	89	54		
316.72	317.00	40.7	38.7	2.0	BB	2	Y	34	214	184	224		
334.60	334.95	40.6	38.8	1.8	BB	1	Y	69	69	39	119		
362.63	363.25	39.7	38.8	0.9	MF	2	Y	157	157	101	239		
365.06	365.20	41.7	38.9	2.8	BB	3	Y	66	246	226	264		
371.26	372.40	42.3	38.9	3.4	BB	3	Y	41	221	209	247		
372.80	376.71	38.9	38.8	0.1	MF	3	N	48	48	32	78		
386.44	386.64	40.0	38.8	1.2	BB	3	Y	34	214	209	224		
388.57	389.52	46.8	38.7	8.1	WO	3	Y	61	241	215	267		
398.00	398.91	39.2	38.9	0.3	BB	2	Y	27	207	159	249		
643.74	643.96	39.5	38.8	0.7	KS	2	Y	32	32	14	48		
650.98	651.09	39.5	38.9	0.6	BB	3	N	51	231	191	271		
659.85	660.54	42.0	38.7	3.3	BB	2	N	5	5	-5	95		
682.82	690.07	38.8	38.7	0.1	MF	3	N	74	74	45	90		
716.43	717.50	43.1	39.3	3.8	BB	2	Y	59	239	211	269		
721.15	728.90	38.9	38.8	0.1	MF	2	N	50	50	10	100		
752.59	767.77	38.9	38.8	0.1	MF	2	Y	45	45	0	90		
777.34	779.70	38.9	38.8	0.1	MF	2	Y	58	58	10	90		
790.40	793.58	38.9	38.8	0.1	MF	2	Y	64	64	0	110		
793.62	793.81	40.0	38.8	1.2	BB	2	Y	55	235	189	289		
803.74	803.87	39.3	38.8	0.5	BB	3	Y	29	209	187	219		
813.73	813.85	39.5	38.9	0.6	BB	1	Y	11	11	344	34		
878.98	909.70	39.0	38.9	0.1	MF	1	N	69	0	360			
883.00	885.20	39.3	38.9	0.4	BB	3	N	44	224	129	241		
888.80	892.80	39.1	38.9	0.2	BB	3	N	39	219	189	229		
896.26	896.49	39.3	38.9	0.4	BB	3	Y	63	243	213	267		
923.18	923.54	39.3	39.1	0.3	BB	2	N	15	15	321	69		
944.09	946.90	40.7	39.1	1.7	BB	2	Y	171	171	115	231		
970.00	979.37	39.1	39.0	0.1	MF	3	N	52	52	0	360		
970.70	974.90	42.4	39.0	3.5	BB	3	N	11	11	343	47		
978.23	978.87	40.2	39.1	1.1	BB	2	N	39	219	183	244		
989.00	989.30	47.1	39.1	8.0	BB	3	Y	51	231	197	257		

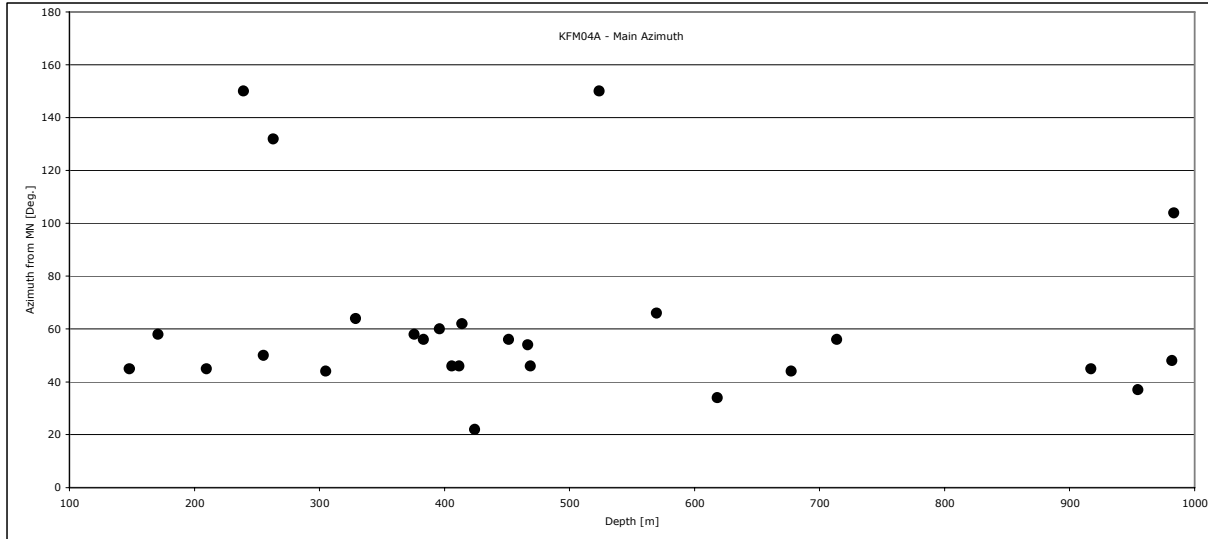


## KFM03B



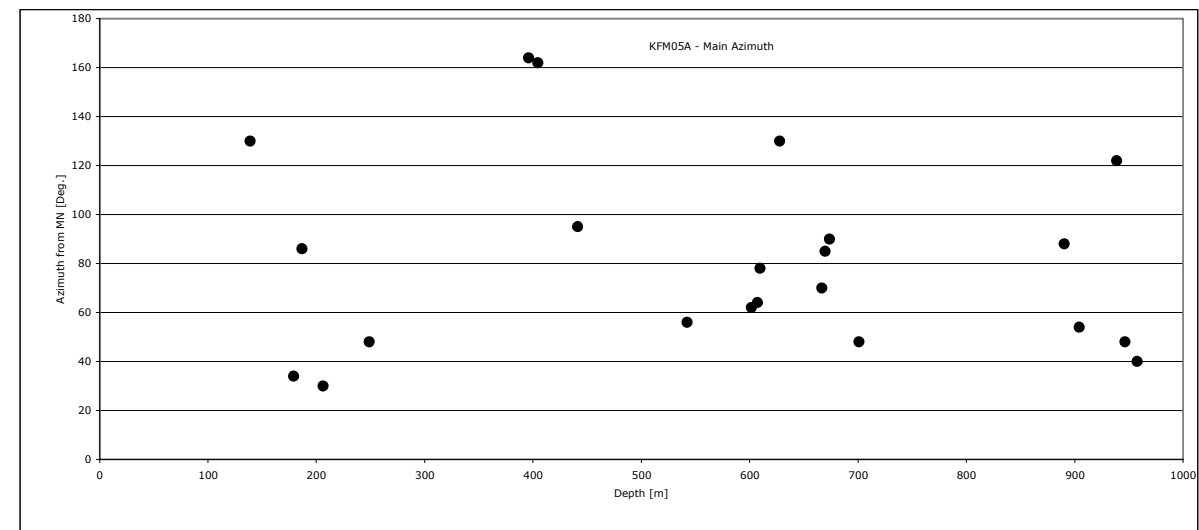
## KFM04A

KFM04A - Observed BB, WO, KS and MF													
Top Depth	Bot. depth	Max R	Median R	dRmax	Class	Uncertainty	Cross. struct.	Main Azimuth	Azimuth	Aperture a1	Aperture a2	Comments	
[m]	[m]	[mm]	[mm]	[mm]		[0-3]	[Yes/No]	[° from MN]	[° from MN]	[° from MN]	[° from MN]		
148.04	148.47	41.0	38.8	2.2	WO	2	?	45	45	0	360	Larger fallouts	
170.98	171.93	41.1	38.8	2.3	KS	2	Y	58	238	214	264		
209.60	209.84	40.0	39.0	1.0	BB	2	Y	45	45	-44	124		
239.30	239.90	55.0	39.5	15.5	BB	1	Y	150	150	80	215		
240.26	247.62	44.0	39.4	4.6	MF	1	Y			0	360		
255.18	256.00	60.0	38.8	21.2	BB	3	?	50	50	0	106		
262.92	263.54	55.0	38.8	16.2	KS	2	Y	132	132	18	244		
305.00	311.01	42.0	38.7	3.3	BB	3	N	44	44	-32	90		
328.99	329.34	42.1	38.6	3.5	BB	1	Y	64	64	28	84		
359.51	359.86	102.0	38.7	63.3	WO	2	Y						
375.85	376.89	41.2	38.4	2.8	BB	2	Y	58	58	42	72		
383.12	383.44	41.8	38.6	3.2	BB	1	Y	56	56	42	74		
396.11	400.78	48.7	38.5	10.2	BB	2	Y	60	60	44	90	7 small BB	
405.87	407.38	48.0	38.3	9.7	BB	3	N	46	46	10	104		
411.75	412.65	41.3	38.5	2.8	BB	3	Y	46	46	0	68		
414.04	414.45	60.0	38.5	21.5	BB	3	Y	62	62	30	104		
414.50	419.54	41.0	38.5	2.5	MF	2	Y			0	360	Larger fallouts	
424.17	425.82	40.7	38.5	2.2	BB	2	N	22	202	178	272		
440.32	450.43	39.5	38.5	1.0	MF	1	N			0	360	Larger fallouts	
451.35	459.50	50.0	38.5	11.5	BB	1	Y	56	56	0	90	Several small BB	
466.60	466.87	41.0	38.5	2.5	BB	2	Y	54	234	208	256		
468.70	468.86	41.2	38.4	2.8	BB	2	Y	46	46	12	86		
523.68	524.48	41.1	38.4	2.7	BB	1	Y	150	150	120	180		
569.65	570.00	44.6	38.4	6.2	BB	2	y	66	66	20	104		
618.21	618.51	42.1	38.4	3.8	BB	2	Y	34	214	178	246		
645.34	681.40	38.6	38.5	0.1	MF	2	N			0	360		
677.29	678.17	41.0	38.6	2.4	BB	2	Y	44	224	208	244		
713.80	714.99	38.6	38.5	0.1	MF	2	N	56	236	208	256		
717.16	719.27	38.6	38.5	0.1	MF	2	N			0	360		
773.00	779.00	38.6	38.5	0.1	MF	2	N			0	360		
897.20	899.95	38.5	38.4	0.1	MF	2	N			0	360		
916.88	917.76	46.0	38.6	7.5	BB	2	Y	45	45	-40	100		
954.50	954.75	48.0	38.6	9.4	WO	1	Y	37	217				
981.76	982.22	54.0	38.7	15.3	BB	1	Y	48	48	-30	145		
983.32	984.11	55.0	38.7	16.3	KS	1	Y	104	284	180	145		



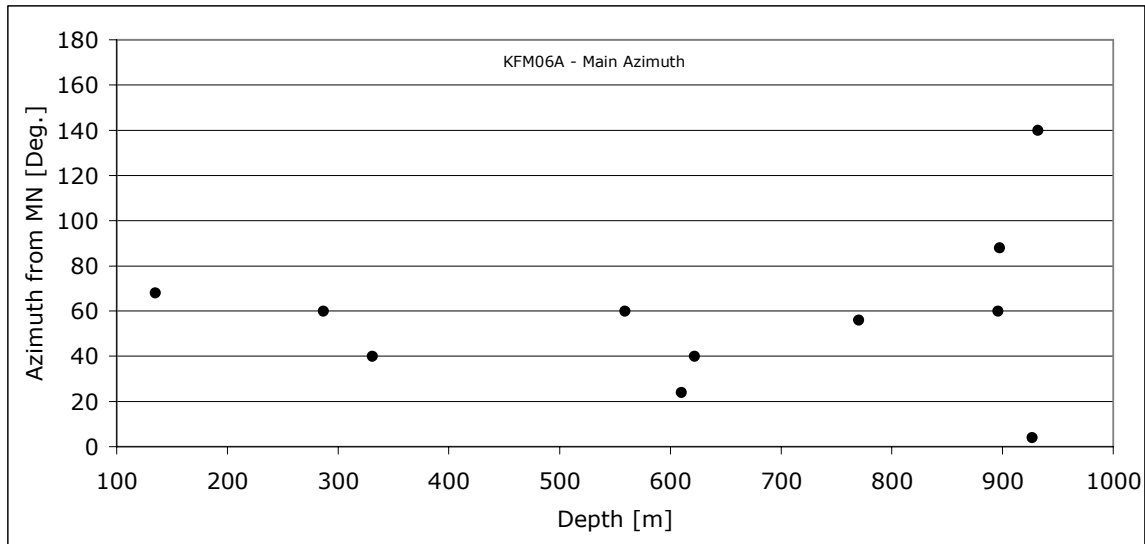
## KFM05A

KFM05A - Observed BB, WO, KS and MF													
Top Depth [m]	Bot. depth [m]	Max R [mm]	Median R [mm]	dRmax [mm]	Structure	Uncertainty [0-3]	Cross. struct. [Yes/No]	Main Azimuth [° from MN]	Azimuth [° from MN]	Aperture a1 [° from MN]	Aperture a2 [° from MN]	Comments	
139.00	140.30	38.8	38.7	0.1	BB	1	Y	130	130	110	210		
179.15	180.40	46.0	38.6	7.4	BB	2	Y	34	214	180	250		
186.80	188.40	38.7	38.6	0.1	BB	2	Y	86	266	234	302		
206.24	209.00	45.7	38.7	7.0	BB	2	Y	30	30	-90	68		
248.90	249.00	44.1	38.6	5.5	BB	2	Y	48	228	178	256		
396.00	396.80	38.6	38.5	0.1	BB	1	Y	164	164	124	202		
404.59	407.14	38.6	38.5	0.1	MF	1	Y	162	162	112	222		
441.40	442.25	40.0	38.5	1.6	BB	1	Y	95	95	58	162		
542.23	543.22	38.4	38.3	0.1	MF	2	N	56	236	198	258		
601.68	603.48	38.2	38.1	0.1	MF	2	Y	62	242	200	262		
607.30	607.80	42.1	38.7	3.4	BB	3	Y	64	64	42	126		
609.60	613.60	50.5	38.5	12.0	BB	3	Y	78	78	26	124		
627.77	628.12	40.0	38.4	1.6	BB	1	Y	130	130	114	144		
666.60	667.60	42.5	35.5	7.0	BB	3	Y	70	70	40	134		
669.80	671.35	41.2	38.7	2.4	BB	2	Y	85	85	76	146		
673.73	674.08	40.0	38.7	1.3	BB	2	Y	90	90	60	140		
701.00	702.21	43.2	38.4	4.8	BB	3	Y	48	228	200	250		
713.50	720.10	103.0	38.5	64.5	WO	1	Y						
890.50	895.20	42.3	38.8	3.6	BB	3	N	88	88	48	112	Consisting of 3 BB	
904.25	904.65	40.3	38.7	1.6	BB	2	Y	54	54	30	80		
904.66	916.84	38.5	38.4	0.1	MF	2	N			0	360		
934.70	965.00	38.6	38.5	0.1	MF	2	N			0	360		
938.80	939.50	39.0	38.7	0.3	KS	2	Y	122	122	64	180		
946.50	946.80	78.7	38.8	40.0	KS	2	Y	48	48	-30	108		
957.70	958.00	44.5	38.8	5.7	BB	3	N	40	220	200	258		
978.40	979.60	76.0	38.8	37.2	WO	2	N						



## KFM06A

KFM06A - Observed BB, WO, KS and MF													
Top Depth [m]	Bot. depth [m]	Max R [mm]	Median R [mm]	dRmax [mm]	Structure	Uncertainty [0-3]	Cross. struct.	Main Azimuth [° from MN]	Azimuth [° from MN]	Aperture α1 [° from MN]	Aperture α2 [° from MN]	Comments	
135.00	136.30	44.8	38.8	6.1	BB	3	N	68	68	40	92		
286.64	288.31	48.7	39.0	9.7	BB	3	N	60	60	16	84		
331.00	337.00	38.7	38.6	0.1	MF	3	N	40	40	-10	80		
559.02	559.28	86.0	38.4	47.6	BB	2	Y	60	240	200	256		
610.07	611.10	38.2	38.1	0.1	MF	3	N	24	24	-20	68		
621.82	622.94	38.2	38.1	0.1	MF	2	Y	40	40	16	60		
770.10	770.90	86.0	38.4	47.6	WO	1	Y	56	236	164	272		
876.20	876.42	45.8	38.5	7.3	WO	2	Y			0	360		
895.80	896.00	47.1	38.4	8.8	KS	1	N	60	240	192	296		
897.20	898.00	42.0	38.3	3.7	BB	2	Y	88	88	48	144		
926.60	929.30	45.4	38.4	7.0	BB	2	Y	4	184	108	236		
931.90	932.50	44.6	38.6	6.0	KS	1	Y	140	320	288	348		



## KFM07C

KFM07C - Observed BB, WO, MF and KS												
Top Depth [m]	Bot. depth [m]	Max R [mm]	Median R [mm]	dRmax [mm]	Class	Uncertainty [0-3]	ross. struc [Yes/No]	ain Azimut [° from MN]	Azimuth [° from MN]	Aperture a1 [° from MN]	Aperture a2 [° from MN]	Comments
102.32	103.14	44.0	38.1	5.9	BB	3	Y	50	50	0	100	
122.90	123.17	39.1	38.0	1.1	BB	3	Y	22	202	175	230	
161.05	162.45	38.1	38.0	0.1	MF	3	N	46	226	196	266	
163.50	166.50	38.1	38.0	0.1	MF	2	N	46	226	170	252	
168.95	173.28	38.1	38.0	0.1	MF	3	N	46	46	0	360	
179.25	188.00	38.1	38.0	0.1	MF	3	Y	50	230	186	268	
189.92	192.11	38.1	38.0	0.1	MF	3	N	58	238	192	274	
197.94	205.04	38.1	38.0	0.1	MF	3	N	50	230	196	264	
209.00	218.00	38.1	38.0	0.1	MF	3	N	54	234	200	270	
229.98	237.78	38.1	38.0	0.1	MF	3	N	54	234	200	270	
239.19	254.75	38.1	38.0	0.1	MF	3	N	54	234	200	270	
266.65	275.25	38.0	37.9	0.1	MF	3	N	46	226	200	272	
275.25	275.75	39.3	37.8	1.5	BB	3	Y	34	214	192	238	
275.75	283.12	38.0	37.9	0.1	MF	3	N	60	240	198	262	
285.38	293.54	38.0	37.9	0.1	MF	3	N	52	232	208	260	
293.54	296.07	38.8	37.8	1.0	BB	3	Y	42	42	12	70	2 BB
296.07	302.27	37.9	37.8	0.1	MF	3	N	60	240	202	268	
305.00	310.39	37.9	37.8	0.1	MF	2	N			0	360	
310.99	311.51	40.7	37.9	2.8	BB	3	Y	90	90	36	132	
318.35	320.27	37.9	37.8	0.1	MF	3	N	66	246	180	290	
320.39	320.71	50.0	37.8	12.2	BB	3	N	30	210	148	254	
320.71	325.00	37.9	37.8	0.1	MF	2	N	68	248	206	288	
325.00	335.25	37.9	37.8	0.1	MF	3	N	56	236	0	360	
335.28	347.30	38.2	37.8	0.4	BB	1	Y	90	90	24	124	Several small BB or just MF
347.40	349.20	51.0	37.8	13.2	WO	2	Y	64	244	0	360	
348.82	356.74	38.4	37.6	0.8	MF	3	Y	50	50	0	90	Or small BB
356.75	357.82	61.0	37.6	23.4	WO	2	Y	24	204	0	360	
357.98	360.04	37.8	37.7	0.1	MF	2	N	60	240	194	276	
360.07	360.32	48.0	37.7	10.3	KS	2	N	0	180	130	214	
360.32	364.79	37.8	37.7	0.1	MF	3	N	34	214	188	258	
364.79	366.28	45.0	37.7	7.3	BB	2	Y	48	48	28	78	2 small BB
366.75	367.52	44.0	37.7	6.3	BB	3	Y	64	64	24	122	
368.87	372.11	38.4	37.7	0.7	BB	1	T	62	242	0	286	3-4 small BB or just MF
372.11	411.63	37.8	37.7	0.1	MF	3	N	44	224	0	360	
412.65	416.06	37.8	37.7	0.1	MF	3	N	50	230	194	272	
424.59	427.89	37.8	37.7	0.1	MF	3	N	84	264	224	298	
427.90	430.45	41.3	37.7	3.6	BB	3	N	70	70	30	100	Partly covered by PLEX stabilisat
431.59	433.31	37.9	37.8	0.1	MF	2	N	54	234	208	262	
433.71	434.22	40.0	37.8	2.2	BB	2	Y	72	252	204	282	
435.00	482.00	37.8	37.7	0.1	MF	3	N	58	238	200	268	
490.21	491.23	40.7	37.6	3.1	BB	3	Y	42	222	185	268	
491.27	492.11	37.7	37.6	0.1	MF	2	N	56	236	200	270	
492.14	493.15	37.9	37.6	0.3	BB	2	Y	64	244	214	276	

